

RadioRAG: Online Retrieval-augmented Generation for Radiology Question Answering

Soroosh Tayebi Arasteh (1,2,3,4), Mahshad Lotfinia (1), Keno Bressemer (5,6), Robert Siepmann (1), Lisa Adams (6), Dyke Ferber (7,8), Christiane Kuhl (1), Jakob Nikolas Kather (7,8,9), Sven Nebelung (1), Daniel Truhn (1)

- (1) Department of Diagnostic and Interventional Radiology, University Hospital RWTH Aachen, Aachen, Germany.
- (2) Pattern Recognition Lab, Friedrich-Alexander-Universität Erlangen-Nürnberg, Erlangen, Germany.
- (3) Department of Urology, Stanford University, Stanford, CA, USA.
- (4) Department of Radiology, Stanford University, Stanford, CA, USA.
- (5) Institute for Radiology and Nuclear Medicine, German Heart Centre Munich, Technical University of Munich, Munich, Germany.
- (6) Department of Radiology, Klinikum rechts der Isar, Technical University of Munich, Munich, Germany.
- (7) Else Kroener Fresenius Center for Digital Health, Faculty of Medicine and University Hospital Carl Gustav Carus, TUD Dresden University of Technology, Dresden, Germany
- (8) Medical Oncology, National Center for Tumor Diseases (NCT), University Hospital Heidelberg, Heidelberg, Germany.
- (9) Department of Medicine I, Faculty of Medicine and University Hospital Carl Gustav Carus, TUD Dresden University of Technology, Dresden, Germany.

Correspondence

Soroosh Tayebi Arasteh, Dr.-Ing., Dr. rer. medic.
Department of Diagnostic and Interventional Radiology,
University Hospital RWTH Aachen
Pauwelsstr. 30
52074 Aachen, Germany
soroosh.arasteh@rwth-aachen.de

This is a preprint version.
The paper is published in Radiology: Artificial Intelligence. RSNA

S. Tayebi Arasteh, M. Lotfinia, K. Bressemer, et al. "RadioRAG: Online Retrieval-augmented Generation for Radiology Question Answering." *Radiology: Artificial Intelligence*, (2025), 7(4):e240476. DOI: <https://doi.org/10.1148/ryai.240476>

Abstract

Large language models (LLMs) often generate outdated or inaccurate information based on static training datasets. Retrieval-augmented generation (RAG) mitigates this by integrating outside data sources. While previous RAG systems used pre-assembled, fixed databases with limited flexibility, we have developed Radiology RAG (RadioRAG), an end-to-end framework that retrieves data from authoritative radiologic online sources in real-time. We evaluate the diagnostic accuracy of various LLMs when answering radiology-specific questions with and without access to additional online information via RAG. Using 80 questions from the RSNA Case Collection across radiologic subspecialties and 24 additional expert-curated questions with reference standard answers, LLMs (GPT-3.5-turbo, GPT-4, Mistral-7B, Mixtral-8x7B, and Llama3 [8B and 70B]) were prompted with and without RadioRAG in a zero-shot inference scenario. RadioRAG retrieved context-specific information from www.radiopaedia.org in real-time. Accuracy was investigated. Statistical analyses were performed using bootstrapping. The results were further compared with human performance. RadioRAG improved diagnostic accuracy across most LLMs, with relative accuracy increases ranging up to 54% for different LLMs. It matched or exceeded non-RAG models and the human radiologist in question answering across radiologic subspecialties, particularly in breast imaging and emergency radiology. However, the degree of improvement varied among models; GPT-3.5-turbo and Mixtral-8x7B-instruct-v0.1 saw notable gains, while Mistral-7B-instruct-v0.2 showed no improvement, highlighting variability in RadioRAG's effectiveness. LLMs benefit when provided access to domain-specific data beyond their training data. RadioRAG shows potential to improve LLM accuracy and factuality in radiology question answering by integrating real-time domain-specific data.

1. Introduction

Artificial intelligence (AI) is in the process of changing diagnostic radiology by enhancing image analysis, improving diagnostic accuracy, and streamlining workflow processes¹. Recent advances in large language models (LLMs)²⁻⁴ have demonstrated potential in extracting structured information from radiological reports^{5,6}, enhancing data mining capabilities⁷, improving diagnostic accuracy^{6,8}, and enabling more reliable speech recognition⁹. However, the use of LLMs in radiology comes with challenges, most prominently the risk of generating inaccurate information and perpetuating biases¹⁰⁻¹². Strategies like human feedback¹³ and prompt engineering have been employed to refine outputs but ultimately cannot solve the problem^{1,14,15}. This is due to the fact that LLMs have to rely on their internal knowledge which is incomplete and may be biased. Rather, it was proposed that LLMs should be used as reasoning engines¹⁶ with access to external sources that they can access. This approach is called retrieval-augmented generation (RAG)¹⁷ and may remedy two problems: firstly, the risk of hallucinating information is reduced, since source material can be used and cited¹⁸. Secondly, LLMs can access up-to-date information through RAG, while conventional LLM querying has to rely on the information fed to the model during training.

Recent studies have demonstrated the effectiveness of RAG in answering general clinical questions^{19,20}. However, its application in radiology has not been explored. In this study, we introduce Radiology RAG (RadioRAG) as a novel framework tailored specifically for typical inquiries in diagnostic radiology.

RadioRAG employs LLMs as reasoning engines to process user questions. It determines which external sources to query for relevant information, collects the source data, and then compiles a comprehensive answer for the user. Most existing solutions that employ RAG use static, pre-compiled literature databases^{19,20}. In contrast, RadioRAG accesses up-to-date information from radiopaedia²¹ to collect its source data. For more information about Radiopaedia's update frequency, please visit <https://radiopaedia.org/terms>. This architecture enables real-time gathering of contextually relevant information and constructing the database. To our knowledge, RadioRAG is the first implementation of this paradigm in radiology. The hypothesis that we investigated were: 1) the real-time context retrieval system reduces the occurrence of hallucinations and 2) RadioRAG improves the accuracy of LLM responses to detailed questions.

2. Materials and Methods

This retrospective study was conducted in compliance with the Declaration of Helsinki and the relevant guidelines and regulations. The study protocol was approved by the Institutional Review Board (IRB) of the Medical Faculty of RWTH Aachen University (No. EK 028/19).

2.1. RSNA Cases

The existing datasets for medical (QA) answering, such as MultiMedQA¹¹, MedMCQA²², and PubMedQA²³, focus on general medicine and do not cater to the specific needs of diagnostic radiology. To address this gap, we created a tailored dataset, RSNA-RadioQA, using 80 peer-reviewed cases from the Radiological Society of North America (RSNA) Case Collection (<https://cases.rsna.org/>). STA, ML, and DT, with 6, 2, and 14 years of experience, respectively, curated the RSNA-RadioQA dataset. Our dataset covers 18 radiology subspecialties, with at least 5 cases per subspecialty in most cases, prioritizing the most recently published cases. Questions were created by providing the clinical history from the RSNA’s case description along with the image characteristics as described in the figure caption. Since we concentrated on LLM without image processing capabilities, the image itself was not provided. Care was taken to exclude any differential diagnoses provided for the case. **Figure 1** illustrates a typical example for such a question. **Table 1** provides detailed information on the full RSNA-RadioQA dataset. We make this dataset available as open-source in **Appendix S1**.

2.2. Expert-Curated Cases

Data contamination is a significant challenge that arises when LLMs are trained on widely sourced web data that might include the datasets used for their evaluation^{19,24}. Although solutions like ClinicalQA¹⁹ have attempted to address these gaps in the general medical domain, a radiology-specific dataset had been lacking.

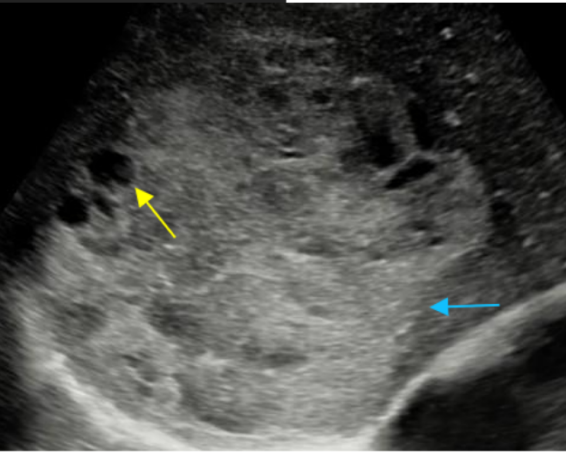
We therefore developed an additional dataset of 24 typical questions in radiology that we call ExtendedQA. These questions were carefully crafted by a radiologist (RS with 5 years of experience and a specialty in diagnostic and interventional radiology). The questions were validated by another board-certified radiologist (DT with 14 years of experience and a specialty in diagnostic and interventional radiology). The complete ExtendedQA dataset is available as open-access in **Appendix S2**.

2.3. System Design

Figure 2 gives an overview over the design of RadioRAG in an end-to-end framework. The following sections detail each component of the process. A glossary of key technical terms can be found in **Appendix S3**.

Table 1: Characteristics of the datasets used in the study. For more details about the RSNA-RadioQA and ExtendedQA datasets, refer to **Appendices S1** and **S2**. *The youngest patient was a 2-day old baby. SD: Standard deviation, N/A: Not available.

Dataset	RSNA-RadioQA	ExtendedQA
Patient age [years]		
Median	44	N/A
Mean \pm SD	44 \pm 21	
Range	(0*, 80)	
Patient sex [n (%)]		
Total	80 (100%)	N/A
Female	37 (46%)	
Male	43 (54%)	
Number of questions per subspecialty [n (%)]		
Total	80 (100%)	24 (100%)
Breast Imaging	10 (12%)	0 (0%)
Cardiac	8 (10%)	2 (8%)
Chest	13 (16%)	7 (29%)
Computed Tomography	28 (35%)	7 (29%)
Emergency Radiology	6 (8%)	3 (13%)
Gastrointestinal	12 (15%)	6 (25%)
Genitourinary	8 (10%)	1 (4%)
Head and Neck	9 (11%)	1 (4%)
Magnetic Resonance Imaging	20 (25%)	7 (29%)
Molecular Imaging	11 (14%)	0 (0%)
Musculoskeletal	14 (18%)	6 (25%)
Neuroradiology	11 (14%)	0 (0%)
Nuclear Medicine	13 (16%)	0 (0%)
Oncologic Imaging	16 (20%)	0 (0%)
Pediatric	7 (9%)	1 (4%)
Radiation Oncology	9 (11%)	0 (0%)
Ultrasound	10 (12%)	0 (0%)
Vascular Imaging	13 (16%)	3 (13%)



Image/Video details

Figure legend:

Axial proton-density weighted MR image with fat suppression through the right thigh above the level of the knee shows a hyperintense 13 cm mass with multiple low-intensity internal septations (blue arrow) deep to the vastus musculature (yellow arrow). The mass is anterior to and partially encasing the distal femoral diaphysis (white arrow). There is no cortical disruption to suggest osseous invasion.

- Clinical information

Age and gender: 56 year old male

Clinical history & presentation: 6-year-old male presented with 3-months history of off and on fever relieved by medication, weight loss, and constipation.

Pathology: Ultrasound guided biopsy was performed using 18G and 16 cm needle and sample sent for the histopathological analysis. Macroscopic appearance revealed well circumscribed mass showing cystic -necrotic areas containing hemorrhage as well as myxoid matrix. Microscopic examination revealed atypical spindle like cells showing repetitive mitotic figures and positivity for vimentin staining.

Physical exam: On physical examination, the liver was palpable 5-6 cm below the costal margin, firm in consistency, and moving proportionately with respiration. No redness over right hepatic region. Localized tenderness present. The spleen was not palpable. There were no palpable lymph nodes.

Other diagnostic testing: Serum AFP levels were <1.3 ng/ml.

LLM

RSNA-RadioQA-Q37

You are a helpful expert medical research assistant. Answer the following question. Use one sentence only and keep the answer concise:

Question: A 6-year-old male presented with a 3-month history of off-and-on fever relieved by medication, weight loss, and constipation. Ultrasound-guided biopsy was performed using 18G and 16 cm needle and the sample was sent for histopathological analysis. Macroscopic appearance revealed a well-circumscribed mass showing cystic-necrotic areas containing hemorrhage as well as a myxoid matrix. Microscopic examination revealed atypical spindle-like cells showing repetitive mitotic figures and positivity for vimentin staining. A transverse grey-scale ultrasound image of the abdomen in a supine position shows a large heterogeneously hyperechoic mass. It occupies the entire right lobe of the liver involving segments V, VI, VII, and VIII. The mass shows hyperechoic and anechoic cystic components within. What is the most likely diagnosis?

Figure 1: RSNA-RadioQA dataset generation. The image is shown for context only; no images were included in this study. The screenshot is taken from a peer-reviewed case from RSNA Case Collection in²⁵, with the question ID: RSNA-RadioQA-Q37.

2.3.1. Browser and the Database

To investigate the reasoning capabilities of the LLMs in our study, we isolated automated query generation and matching to external sources by using the same model for all LLMs: using GPT-3.5-turbo via its API, the system extracts up to five search key-phrases from a given radiological question. The threshold of five was chosen experimentally, as we observed that relevant sources

were always found within the first five searches of radiopaedia, minimizing unnecessary searches and reducing system response time. The prompt specified to GPT-3.5-turbo is: "You are a helpful expert medical research assistant. I have a medical question, particularly in the field of radiology. Please summarize the question to extract the most representative keywords for use in online scientific article searches. Return a maximum of five keywords that are scientifically relevant to radiology." Two examples were provided to the model within the prompt, as shown in **Figure 2B** (two-shot approach). For each question, the same set of key-phrases was used for all RadioRAG-powered LLMs to ensure a fair comparison.

After acquiring relevant search keywords, the model searches through articles on www.radiopaedia.org, selecting the five articles most pertinent to each keyword. As part of our validation process, STA and DT reviewed the final selected articles to ensure their appropriateness. These articles are then segmented into chunks of 1,000 tokens, each with a 200 token overlap. Each chunk is converted into a vector using the 'text-embedding-ada-002' embedding function from OpenAI and temporarily stored in a vector database managed by Chroma (<https://www.trychroma.com/>).

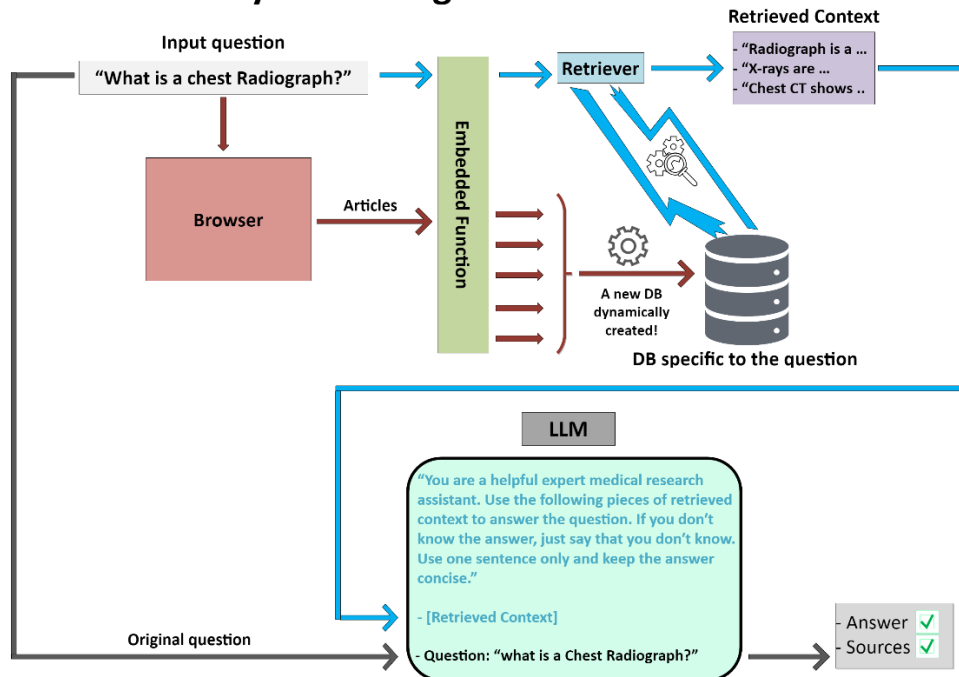
2.3.2. Retriever

With the database prepared, the original query is also embedded into a vector using the same embedding function. This query vector is then compared against all vectors in the database using cosine similarity to retrieve the top three most similar vectors ($k=3$). These vectors are matched to their textual form, and the relevant text is prepared for the next stage. The LangChain framework is used for this retrieval process.

2.3.4. Large Language Model (LLM)

The final stage involves the respective LLM under investigation, which receives the original query along with the contextually relevant text fragments retrieved in the previous step. The LLM is instructed to provide a concise answer in one sentence, based solely on the provided context. If the answer is unknown, the LLM must explicitly state this. We used the following prompt: "Use the following pieces of retrieved context to answer the question. If you don't know the answer, say 'I don't know.' Answer concisely in one sentence." This process contrasts with traditional LLM QA methods that involve responding to queries without additional context, typically prompted with: "You are a helpful expert medical research assistant. Answer the following question concisely in one sentence". To ensure reproducibility, a temperature value of 0 was set for all LLM responses, except for those involving Mistral and Mixtral models, where a minimum temperature of 0.1 was necessary (for which we set it at 0.1). A top-p value of 1 was consistently used across all cases. Through this choice, provided results were reproducible for the same model version.

A RadioRAG System Design



B Browser

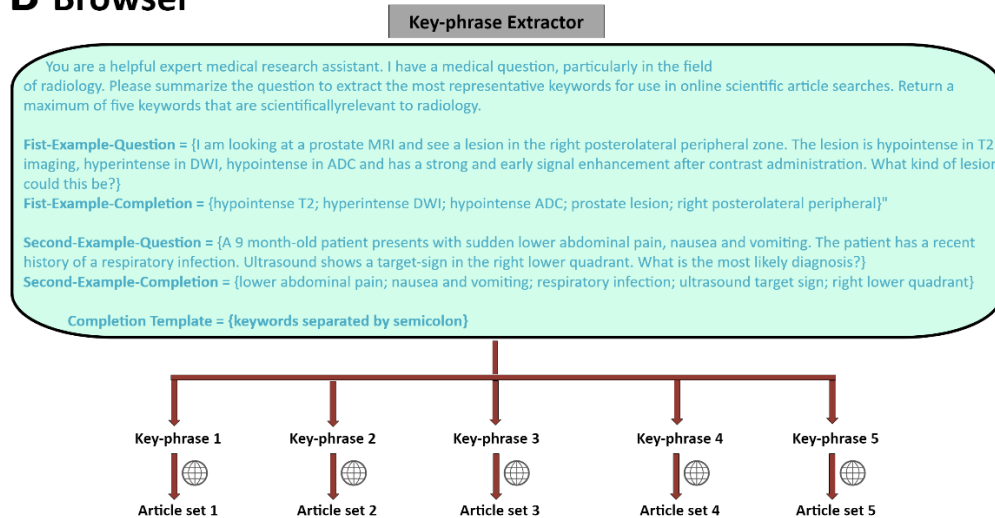


Figure 2: Radiology Retrieval Augmented Generation (RadioRAG) architecture overview. (A) Shows that RadioRAG system design. Initially, the input question is analyzed and the relevant articles are retrieved using the “Browser” module, which are then chunked into multiple documents. These documents are converted into vector representations and stored in a dynamically created, on-the-fly vector database (DB) for each query. The question is embedded using the same function and its vector compared against the DB vectors using cosine distance to select the closest three vectors. These vectors are reverted to their textual form to create the context for the final step. The LLM then receives the original question along with this context and is directed to use the context to formulate an answer. **(B)** Shows the architecture of the Browser module. After analyzing the input question, the 5 most representative key-phrases are extracted using the key-phrase extractor, implemented with GPT-3.5-turbo in our examples. Each key-phrase triggers the retrieval of relevant articles from www.radiopaedia.org.

2.4. Evaluation

STA and DT performed the evaluation. To assess the efficacy of RadioRAG across varying scales of language models, we tested both smaller and larger LLMs. All final LLM responses for this study were generated between April 1 and April 25, 2024. We included GPT-3.5-turbo, GPT-4, Mistral-7B-instruct-v0.2, Mistral-8x7B-instruct-v0.1, Llama3-8B, and Llama3-70B-instruct. This set of models represents the state-of-the-art in size and capabilities. Each model was integrated into the RadioRAG pipeline and evaluated in both a conventional QA setup and within the RadioRAG framework.

The performance of all models was evaluated by comparing their responses within the RadioRAG framework to those in conventional QA, using reference standard answers as the benchmark. Although various metrics like naturalness, fluency, and coherence are commonly used in LLM evaluation^{26–28}, we prioritized accuracy^{19,29,30} as the primary metric due to the specific nature of our application, which demands correct and concise diagnostic answers. Accuracy was measured by scoring responses as true (1) if they correctly addressed the query and false (0) otherwise¹⁹. Factuality was also assessed by verifying the suitability of the sources the LLMs cited for each answer. Additionally, the models' ability to recognize and admit when the available information was insufficient was evaluated, requiring them to state "I don't know" in such instances. Any inaccuracies or omissions in expressing uncertainty were considered deviations from expected factuality and transparency.

Moreover, to assess the practical utility of RadioRAG, we compared the diagnostic performance of RadioRAG-powered LLMs to human radiologist on both the RSNA-RadioQA and ExtendedQA datasets. A board-certified radiologists (LA with 9 years of experience and subspecialty in chest and oncologic imaging) was blinded to the reference standard answers, curation of the datasets, and LLM responses. The human expert answered the same set of questions given to the LLMs, based solely on their own knowledge and without accessing any online information or additional materials such as images. The responses were evaluated by STA and DT using the same accuracy metrics applied to the LLMs.

2.5. Statistical Analysis

Statistical analysis was conducted using Python v3.11 with SciPy v1.11, NumPy v1.24, and statsmodels v0.14. packages. To evaluate the variability, separately for each dataset, bootstrapping was employed with 10,000 redraws for the metrics to determine the mean, standard deviation, 95% confidence intervals (CI), and to calculate p-values for differences in accuracy between the RadioRAG and non-RadioRAG setups³¹, ensuring a strictly paired setup where redraws were identical across conditions³². To account for multiple comparisons, the p-values were adjusted for multiplicity using the false discovery rate (FDR). An FDR<0.05 was used.

2.6. Code and Data Availability

All source codes and datasets used in this study are publicly available to ensure transparency and reproducibility. The code has been developed using Python v3.11 with PyTorch v2.1 and is hosted on GitHub at <https://github.com/tayebiarasteh/RadioRAG>. We utilized the LangChain v0.1.0 framework for the RadioRAG pipeline, with Chroma serving as the vector database. The OpenAI API v1.12 provided access to the GPT-4 and GPT-3.5-turbo models as well as the 'text-embedding-ada-002' embedding function from OpenAI. Additionally, the Replicate API v0.25 facilitated cloud execution of Mistral and Mixtral models without local GPU requirements, and Ollama (<https://ollama.com/>) framework for execution of the newly-released Llama3 open-source models. The underlying datasets are publicly accessible and included in the supplemental materials of this publication.

3. Results

3.1. Dataset Characteristics

Mean age over all patients in the RSNA-RadioQA dataset was $44 \pm [SD] 21$ years, with a range of 2 days to 80 years. **Table 1** reports the characteristics of the dataset and the distribution of subspecialties among all questions.

3.2. Impact of RadioRAG on Diagnostic Performance of LLMs

Typical responses of the LLMs to an exemplary question from the RSNA-RadioQA dataset are given in **Table 2**. RadioRAG increased the accuracy of the LLMs' responses on the ExtendedQA dataset as illustrated by **Figure 3**. Detailed results are given in **Table 3**: the accuracy of GPT-3.5-turbo increased from $66\% \pm 5$ (53/80) to $74\% \pm 5$ (59/80) ($P=0.03$), of GPT-4 from $78\% \pm 5$ (62/80) to $79\% \pm 5$ (63/80) ($P=0.28$), of Mixtral-8x7B-instruct-v0.1 from $65\% \pm 5$ (52/80) to $76\% \pm 5$ (61/80) ($P=0.02$), of Llama3-8B from $58\% \pm 6$ (46/80) to $59\% \pm 5$ (47/80) ($P=0.39$), and of Llama3-70B from $66\% \pm 5$ (53/80) to $69\% \pm 5$ (55/80) ($P=0.30$). The only exception was Mistral-7B-instruct-v0.2, which exhibited no change ($55\% \pm 6$ (44/80) in both cases; $P=0.45$). Similarly, for the ExtendedQA dataset, all LLMs demonstrated improvements. In particular, Mixtral-8x7B-instruct-v0.1, Llama3-8B, and Mistral-7B all exhibited significant improvements, while the bigger models also showed improvements, yet without reaching the significance threshold. Detailed results stratified along subspecialties are given in **Table S1**.

3.3. Open-Weights Models Benefit from RadioRAG

While RadioRAG consistently improved diagnostic performance across all tested LLMs, the degree of improvement varied significantly between models. The most complex model, GPT-4 exhibited relative accuracy improvements of 1% [(79-78)/78] and 6% [(75-71)/71], respectively for the two QA datasets, while GPT-3.5-turbo exhibited relative accuracy improvements of 12% [(74-66)/66] and 22% [(71-58)/58], respectively. We observed stronger increases on the ExtendedQA dataset for the open-weights models Mistral-7B-instruct-v0.2 (up to 54% [(71-46)/46], Mixtral-8x7B-instruct-v0.1 (up to 47% [(79-54)/54] and Llama3-8B (up to 34% [(67-50)/50]. Importantly, while open-weights models had inferior performance in the non-RAG setting, RadioRAG rendered these models competitive with GPT-4.

3.4. RadioRAG Enforces Factuality in LLMs

We found that RadioRAG guided the LLMs to ground their answers in factual content from the source data, i.e., whether the provided answer is based on and related to the retrieved context¹⁹. **Table S2** presents detailed quantitative results on hallucination rates for each model. **Tables S3** and **S4** provide overviews of questions, with and without RAG, respectively, using GPT-3.5-turbo as an example.

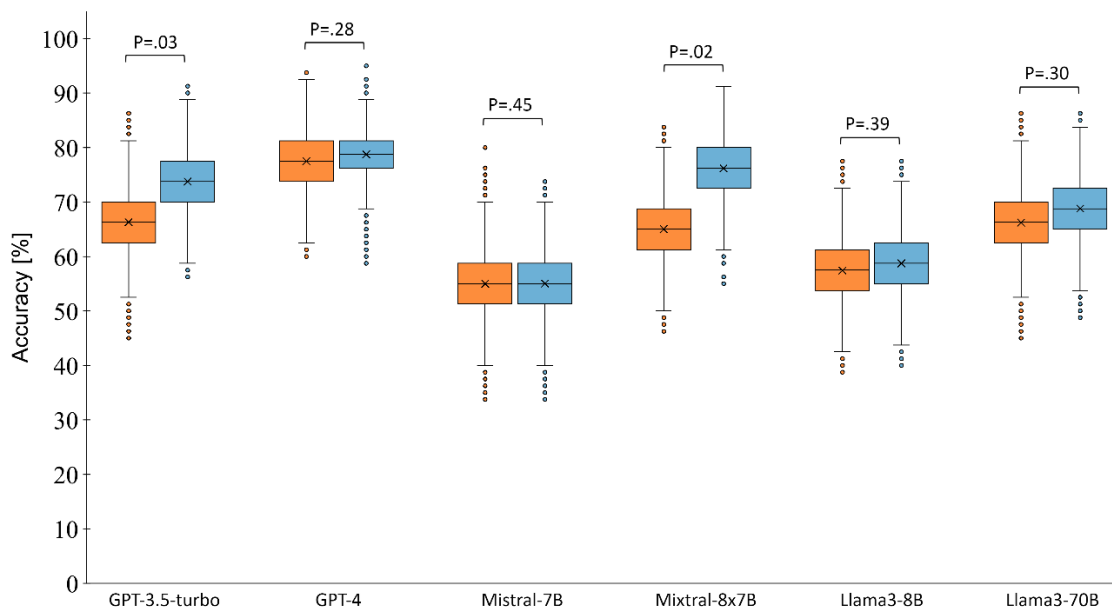
Following the review of the retrieved articles, we generally found that relevant articles were selected in 72% (58/80) of questions for the RSNA-RadioQA dataset and 83% (20/24) for the ExtendedQA dataset. However, in some cases—possibly when a related article was not available on Radiopaedia—unrelated articles were chosen. Additionally, while answers typically aligned closely with the source data, strict adherence occasionally led to inaccuracies when the retrieved articles were not fully relevant to the query, affecting between 15% (12/80) and 20% (16/80) of questions in the RSNA-RadioQA dataset across different LLMs, and between 8% (2/24) and 12% (3/24) of questions in the ExtendedQA dataset for all LLMs. **Table 4** provides an example where the enforcement of factuality resulted in an incorrect answer due to irrelevant context.

This enforcement generally minimized hallucinations by the LLMs; however, different LLMs exhibited varying behavior. For both datasets, Mixtral-8x7B-instruct-v0.1 and GPT-4 showed the fewest hallucinations, with 9% (7/80) and 6% (5/80) for the RSNA-RadioQA dataset, respectively, and 8% (2/24) and 12% (3/24) for the ExtendedQA dataset, respectively.

3.5. Comparison to Human Performance

The human expert radiologist achieved an accuracy of 63% \pm 5 (50/80) (95% CI: 51%, 72%) on the RSNA-RadioQA dataset, which was significantly lower than RadioRAG-powered models of GPT-3.5-turbo (P=0.007), GPT-4 (P=0.001), and Mixtral-8x7B-instruct-v0.1 (P=0.007), but not significantly different from Llama3-70B (P=0.21). It outperformed RadioRAG-powered models of Mistral-7B-instruct-v0.2 (P=0.22) and Llama3-8B (P=0.31). On the ExtendedQA dataset, the radiologist achieved 62% \pm 10 (15/24) (95% CI: 42%, 83%), which was lower than all RadioRAG-powered models, though the differences were not statistically significant (P>0.19).

A RSNA-RadioQA Dataset



B ExtendedQA Dataset

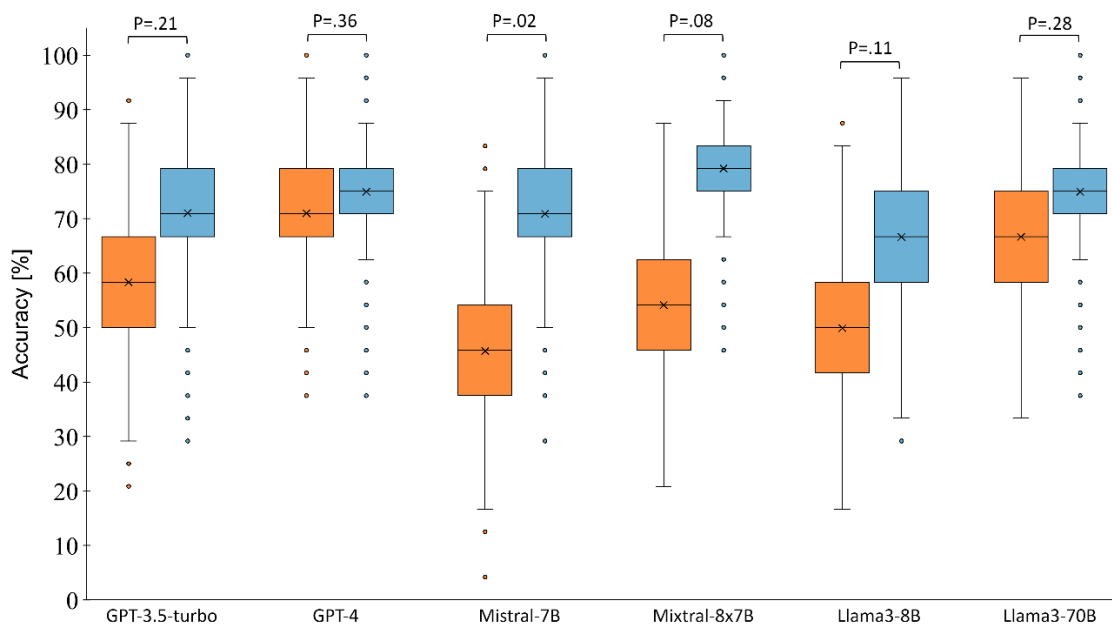


Figure 3: Quantitative evaluation of RadioRAG across datasets. This figure displays the accuracy results on two datasets: **A)** RSNA-RadioQA with $n=80$ (details in **Appendix S1**) and **B)** ExtendedQA with $n=24$ (details in **Appendix S2**). The LLMs included in the evaluation are GPT-3.5-turbo, GPT-4, Mistral-7B-instruct-v0.2 (Mistral-7B), Mixtral-8x7B-instruct-v0.2 (Mixtral-8x7B), Llama3-8B, and Llama3-70B-instruct (Llama3-70B). The orange boxes correspond to the models without using RadioRAG, while the blue boxes correspond to the RadioRAG-powered models. The analysis employs bootstrapping with 10,000 repetitions, allowing replacements. P-values were calculated between each of the RadioRAG-powered methods and their non-RadioRAG counterpart. A value below 0.05 was considered significant.

4. Discussion

In this study, we introduced Radiology RAG (RadioRAG), a novel framework that enhances the diagnostic accuracy of LLMs by utilizing contextually relevant data from an established radiological source. To benchmark RadioRAG, we developed two datasets which we make publicly available: RSNA-RadioQA for internal testing and ExtendedQA as an external dataset.

Overall, our findings show that RadioRAG-powered LLMs outperformed their non-RAG counterparts in most cases, yielding more accurate and reliable outputs in radiological contexts.

To evaluate RadioRAG, we developed RSNA-RadioQA, a diagnostic radiology QA dataset using the RSNA Case Collection. This collection includes peer-reviewed cases from various global institutions and provides a diverse and representative dataset of radiological question answering across multiple subspecialties. However, as these cases had already been published online, there is a potential bias since the LLMs might have previously accessed parts of this data during their training. To mitigate this, we created the ExtendedQA dataset with 24 previously unseen questions as an additional test dataset to confirm the results on RSNA-RadioQA.

In our study, LLMs powered by RadioRAG generally outperformed those in conventional QA setups. GPT-4 excelled in conventional QA settings, but exhibited only slight improvements with RadioRAG. In contrast, LLMs like Mixtral-8x7B-instruct-v0.1, which initially lagged behind in the conventional QA setting, saw substantial gains with RadioRAG, matching or even surpassing GPT-4. This improvement is significant for two key reasons: firstly, it was achieved without additional training, relying solely on strategic guidance during inference—a cost-effective method compared to full model retraining. Secondly, it suggests that high-performance natural language processing may be achievable using open-source LLMs with RAG, potentially reducing reliance on closed-source models like GPT-4.

Previous studies^{19,20,33,34} have applied RAG to medical question answering, yet none have specifically focused on radiology, and except for¹⁹, most have utilized offline RAG where documents from books, articles, and websites are compiled into a static database for retrieval. This approach lacks the immediacy of an online RAG like RadioRAG. By accessing up-to-date information, RadioRAG can adapt to changes in guidelines, image assessment strategies, or updates to imaging techniques.

Table 2: LLM responses to one of the questions, with and without RadioRAG. This exemplary question is chosen from the RSNA-RadioQA dataset (details in **Appendix S1**) with the question ID: RSNA-RadioQA-Q37.

Question	A 6-year-old male presented with a 3-month history of off-and-on fever relieved by medication, weight loss, and constipation. Ultrasound-guided biopsy was performed using 18G and 16 cm needle and the sample was sent for histopathological analysis. Macroscopic appearance revealed a well-circumscribed mass showing cystic-necrotic areas containing hemorrhage as well as a myxoid matrix. Microscopic examination revealed atypical spindle-like cells showing repetitive mitotic figures and positivity for vimentin staining. A transverse grey-scale ultrasound image of the abdomen in a supine position shows a large heterogeneously hyperechoic mass. It occupies the entire right lobe of the liver involving segments V, VI, VII, and VIII. The mass shows hyperechoic and anechoic cystic components within. What is the most likely diagnosis?
Reference Standard Answer	Undifferentiated embryonal sarcoma
RadioRAG Pipeline Key-phrases Source	Key-phrases: fever, weight loss, constipation, ultrasound-guided biopsy, liver mass Most relevant source among the 25 retrieved articles: https://radiopaedia.org/articles/undifferentiated-embryonal-sarcoma-of-the-liver?lang=us
Conventional GPT-3.5-turbo	The most likely diagnosis is hepatoblastoma
RadioRAG+GPT-3.5-turbo	The most likely diagnosis is undifferentiated embryonal sarcoma of the liver.
Conventional GPT-4	The most likely diagnosis for the 6-year-old male with these symptoms and ultrasound findings is a hepatic sarcoma, specifically undifferentiated embryonal sarcoma of the liver (UESL).
RadioRAG+GPT-4	The most likely diagnosis is an undifferentiated embryonal sarcoma of the liver.
Conventional Mistral-7B	The most likely diagnosis is a malignant peripheral nerve sheath tumor (MPNST) or neurofibrosarcoma.
RadioRAG+Mistral-7B-instruct-v0.2	The most likely diagnosis is an undifferentiated embryonal sarcoma of the liver.
Conventional Mixtral-8x7B-instruct-v0.1	The most likely diagnosis is hepatoblastoma, a malignant pediatric liver tumor characterized by atypical spindle-like cells, cystic-necrotic areas, and vimentin positivity, as described in the patient's presentation and ultrasound findings.
RadioRAG+Mixtral-8x7B-instruct-v0.1	The most likely diagnosis is an undifferentiated embryonal sarcoma of the liver, given the patient's age, symptoms, and the ultrasound and histopathological findings.
Conventional Llama3-8B	The most likely diagnosis is a pediatric hepatoblastoma, a rare malignant tumor that originates in the liver, based on the histopathological features and imaging findings.
RadioRAG+Llama3-8B	Undifferentiated embryonal sarcoma of the liver.
Conventional Llama3-70B-instruct	The most likely diagnosis is Undifferentiated Embryonal Sarcoma (UES) of the liver, a rare and aggressive pediatric tumor.
RadioRAG+Llama3-70B-instruct	The most likely diagnosis is undifferentiated embryonal sarcoma of the liver.

Table 3: Statistical analysis results for the RSNA-RadioQA and ExtendedQA datasets. P-values were calculated between each of the RadioRAG-based methods and all the other models. N/A: Not assigned.

Model Name	Accuracy (mean \pm SD [95% CI]) [%]	P-Value					
		RAG+ GPT-3.5-turbo	RAG+ GPT-4	RAG+ Mistral-7B	RAG+Mixtral-8x7B	RAG+Llama3-8B	RAG+Llama3-70B
RSNA-RadioQA Dataset							
RAG+GPT-3.5-turbo	74 \pm 5 [95% CI: 64, 84] (59/80)	N/A	0.07	0.001	0.26	0.005	0.20
RAG+GPT-4	79 \pm 5 [95% CI: 70, 88] (63/80)		N/A	0.001	0.35	0.001	0.02
RAG+Mistral-7B	55 \pm 6 [95% CI: 44, 66] (44/80)			N/A	0.001	0.24	0.005
RAG+Mixtral-8x7B	76 \pm 5 [95% CI: 66, 85] (61/80)				N/A	0.003	0.09
RAG+Llama3-8B	59 \pm 5 [95% CI: 47, 70] (47/80)					N/A	0.05
RAG+Llama3-70B	69 \pm 5 [95% CI: 59, 79] (55/80)						N/A
GPT-3.5-turbo	66 \pm 5 [95% CI: 56, 76] (53/80)	0.03	0.001	0.06	0.04	0.15	0.28
GPT-4	78 \pm 5 [95% CI: 69, 86] (62/80)	0.26	0.28	0.001	0.45	0.001	0.03
Mistral-7B	55 \pm 6 [95% CI: 44, 66] (44/80)	0.001	0.001	0.45	0.001	0.26	0.02
Mixtral-8x7B	65 \pm 5 [95% CI: 55, 75] (52/80)	0.05	0.003	0.06	0.02	0.20	0.26
Llama3-8B	58 \pm 6 [95% CI: 46, 69] (46/80)	0.001	0.001	0.39	0.001	0.39	0.03
Llama3-70B	66 \pm 5 [95% CI: 56, 76] (53/80)	0.07	0.01	0.04	0.04	0.17	0.30
ExtendedQA Dataset							
RAG+GPT-3.5-turbo	71 \pm 9 [95% CI: 50, 88] (17/24)	N/A	0.34	0.44	0.18	0.44	0.36
RAG+GPT-4	75 \pm 9 [95% CI: 58, 92] (18/24)		N/A	0.44	0.34	0.21	0.42
RAG+Mistral-7B	71 \pm 9 [95% CI: 54, 88] (17/24)			N/A	0.28	0.44	0.28
RAG+Mixtral-8x7B	79 \pm 8 [95% CI: 62, 96] (19/24)				N/A	0.27	0.44
RAG+Llama3-8B	67 \pm 10 [95% CI: 46, 83] (16/24)					N/A	0.001
RAG+Llama3-70B	75 \pm 9 [95% CI: 58, 92] (18/24)						N/A
GPT-3.5-turbo	58 \pm 10 [95% CI: 38, 75] (14/24)	0.21	0.11	0.11	0.11	0.28	0.08
GPT-4	71 \pm 9 [95% CI: 50, 88] (17/24)	0.44	0.36	0.44	0.30	0.44	0.34
Mistral-7B	46 \pm 10 [95% CI: 25, 67] (11/24)	0.10	0.01	0.02	0.02	0.08	0.001
Mixtral-8x7B	54 \pm 10 [95% CI: 33, 75] (13/24)	0.18	0.13	0.14	0.08	0.27	0.11
Llama3-8B	50 \pm 10 [95% CI: 29, 71] (12/24)	0.10	0.02	0.04	0.02	0.11	0.001
Llama3-70B	67 \pm 10 [95% CI: 46, 83] (16/24)	0.40	0.30	0.36	0.21	0.44	0.28

Like other RAG systems^{17,19,35}, RadioRAG enforces factual responses from LLMs. Despite this, we found instances where responses were incorrect. This was due to irrelevant context extracted from the sources. Such strict reliance on irrelevant source materials can lead to incorrect answers unless the LLM correctly identifies the irrelevance and states that it does not know the answer. GPT-4 and Llama3-70B-instruct were particularly adept at recognizing when they could not provide informed answers, although they still occasionally failed to do this effectively. Future research should focus on enhancing embedding functions and methodologies to retrieve more relevant context such as fine-tuned embeddings and advanced reranking³⁶, thus minimizing the risk of inaccuracies. Additionally, exploring agentic workflows³⁷, which enable dynamic adjustments based on user input and real-time feedback, could further optimize the system's performance³⁸, allowing the model to balance between retrieved information and its internal knowledge for improved accuracy. Moreover, future work could expand the RadioRAG framework to a multimodal paradigm where images could be included alongside textual data, and a comparison with LLMs that have dynamic web search capabilities (e.g., Perplexity AI, CA, USA) would provide insights into the advantages of controlled retrieval versus real-time web access.

RadioRAG has limitations. First, the on-the-fly generation of a database can be time-consuming, potentially extending the time it takes for RadioRAG to respond compared to conventional QA setups. A comparative analysis of the time required for QA with RadioRAG versus conventional methods is provided in **Appendix S4**. To mitigate this, we have optimized the framework to select up to 5 key-phrases and retrieve 5 articles per key-phrase, resulting in a total of 25 articles. Second, the reliance on continually querying online scientific sources, in our case www.radiopaedia.org, could overload the website, especially if multiple users are accessing it simultaneously, potentially leading to downtimes. Therefore, while RadioRAG offers a compelling proof-of-concept, more research into its efficiency and computational demands is essential before it can be implemented in clinical practice. Future deployments should consider establishing agreements with source websites to ensure fair use and manage the load effectively. Third, the small external ExtendedQA dataset (n=24) limits generalizability. While we used bootstrapping to mitigate this, larger external validations are needed, and we plan to expand the dataset in future work. Future work should validate our findings on larger external datasets. Additionally, we plan to expand the ExtendedQA dataset in future versions to enhance the robustness and generalizability of the results. Fourth, while RadioRAG is adaptable to multiple information sources, in this study, we relied exclusively on Radiopaedia, a well-established source in the radiology community. This reliance on a single source presents a potential limitation, and future studies should consider incorporating additional sources to enhance the system's versatility and accuracy.

In conclusion, RadioRAG introduces real-time data retrieval to enhance the accuracy and factuality of LLMs in radiological diagnostics. This development offers a foundation for further work that could improve diagnostic processes and patient care in healthcare.

Table 4: Factuality and potential hallucinations in RadioRAG. RadioRAG enforces factuality by requiring LLMs to base their responses on the content of retrieved articles. However, strict adherence to these sources can lead to inaccuracies when the context provided is not relevant to the query. In this given example, only GPT-4, powered by RadioRAG, acknowledges the inability to find a relevant answer, while the other RadioRAG-powered LLMs provide incorrect answers, demonstrating potential hallucinations. This exemplary question is chosen from the RSNA-RadioQA dataset with the question ID: RSNA-RadioQA-Q59.

RadioRAG-Powered QA	
Prompt	<p>You are a helpful expert medical research assistant. Use the following pieces of retrieved context to answer the question. If you don't know the answer, just say that you don't know. Use one sentence only and keep the answer concise:</p> <p>- Retrieved Context: <i>Pathology Etiology The majority (80%) of scolioses have no apparent underlying cause and are termed idiopathic 1. Idiopathic scoliosis can be broken down into infantile, juvenile and adolescent based on the age of the patient. The remaining 20% of scolioses are the result of other causes. There are many ways to potentially group these causes, but a simple three-pronged grouping strategy is: neuromuscular: conditions that cause neurological or muscular deficits that result in asymmetric muscular tone resulting in spinal curvature congenital bony: an underlying bony abnormality of the vertebra that results in a relatively fixed spinal curve tumor or treatment: this is a bit of a catch-all for the remainder of causes, most of which relate to an adjacent tumor, or previous treatment, e.g. radiotherapy or cardiac surgery.</i></p> <p><i>Causes neuromuscular scoliosis cerebral palsy Chiari malformation Friedreich ataxia syringomyelia diastematomyelia tethered cord spinal dysraphism muscular dystrophies spinal muscular atrophy connective tissue disorders (e.g. Marfan disease) traumatic paralysis congenital scoliosis segmentation and fusion abnormalities (e.g. hemivertebrae) skeletal dysplasias (e.g. achondroplasia) lumbosacral transitional vertebra tumors bone: osteoid osteoma, osteoblastoma, metastases, neurofibromas in neurofibromatosis type I soft tissues: meningioma, neurofibroma, astrocytoma, ependymoma infection resulting in bony abnormalities (e.g. pyogenic osteomyelitis, tuberculous spondylitis).</i></p> <p>[Source: https://radiopaedia.org/articles/scoliosis]</p> <p>- Question: A 15-year-old male with no significant past medical history presents to orthopedic clinic for evaluation of scoliosis. An abnormality is seen on scoliosis films. Review of systems is positive for frequent nosebleeds. Frontal and lateral views of the spine show dextroconvex thoracic scoliosis with an incidental nodule in the right middle lobe. What is the most likely diagnosis?</p>
Reference Answer	Pulmonary varix
RadioRAG+ GPT-4	Answer: The text does not provide enough information to determine the most likely diagnosis for the 15-year-old male patient.
RadioRAG+ Mixtral-8x7B	Answer: Based on the information provided, the most likely diagnosis is idiopathic scoliosis with an incidental finding of a nodule in the right middle lobe, possibly indicative of a pulmonary condition unrelated to the scoliosis. The frequent nosebleeds may be a clue to this separate condition. However, a definitive diagnosis would require further investigation by a healthcare professional.
RadioRAG+ Llama3-70B	Answer: The most likely diagnosis is neurofibromatosis type 1 (NF1) due to the presence of a spinal curvature and an incidental pulmonary nodule, which are both common features of this genetic disorder.
Conventional QA	
Prompt	<p>You are a helpful expert medical research assistant. Answer the following question. Use one sentence only and keep the answer concise.:</p> <p>- Question: A 15-year-old male with no significant past medical history presents to orthopedic clinic for evaluation of scoliosis. An abnormality is seen on scoliosis films. Review of systems is positive for frequent nosebleeds. Frontal and lateral views of the spine show dextroconvex thoracic scoliosis with an incidental nodule in the right middle lobe. What is the most likely diagnosis?</p>
Conventional GPT-4	Answer: The most likely diagnosis for a 15-year-old male with dextroconvex thoracic scoliosis and an incidental nodule in the right middle lobe, who also experiences frequent nosebleeds, is hereditary hemorrhagic telangiectasia (HHT), also known as Osler-Weber-Rendu syndrome, which is associated with telangiectasias and arteriovenous malformations (AVMs) that can cause pulmonary nodules and epistaxis.
Conventional Mixtral-8x7B	Answer: 15-year-old male with scoliosis, nosebleeds, and a lung nodule may have neurofibromatosis type 1, a genetic disorder often associated with these symptoms.
Conventional Llama3-70B	Answer: The most likely diagnosis is Osler-Weber-Rendu syndrome, a rare genetic disorder characterized by abnormal blood vessel formation and frequent nosebleeds, which can be associated with pulmonary arteriovenous malformations and scoliosis.

Funding Sources

STA was funded and partially supported by the Radiological Cooperative Network (RACOON) under the German Federal Ministry of Education and Research (BMBF) grant number 01KX2021. JNK is supported by the German Cancer Aid (DECADE, 70115166), the German Federal Ministry of Education and Research (PEARL, 01KD2104C; CAMINO, 01EO2101; SWAG, 01KD2215A; TRANSFORM LIVER, 031L0312A; TANGERINE, 01KT2302 through ERA-NET Transcan; Come2Data, 16DKZ2044A; DEEP-HCC, 031L0315A), the German Academic Exchange Service (SECAI, 57616814), the German Federal Joint Committee (TransplantKI, 01VSF21048) the European Union's Horizon Europe and innovation programme (ODELIA, 101057091; GENIAL, 101096312), the European Research Council (ERC; NADIR, 101114631), the National Institutes of Health (EPICO, R01 CA263318) and the National Institute for Health and Care Research (NIHR, NIHR203331) Leeds Biomedical Research Centre. The views expressed are those of the author(s) and not necessarily those of the NHS, the NIHR or the Department of Health and Social Care. This work was funded by the European Union. Views and opinions expressed are however those of the author(s) only and do not necessarily reflect those of the European Union. Neither the European Union nor the granting authority can be held responsible for them. SN and DT were supported by grants from the Deutsche Forschungsgemeinschaft (DFG) (NE 2136/3-1, LI3893/6-1, TR 1700/7-1). DT is supported by the German Federal Ministry of Education (TRANSFORM LIVER, 031L0312A; SWAG, 01KD2215B) and the European Union's Horizon Europe and innovation programme (ODELIA [Open Consortium for Decentralized Medical Artificial Intelligence], 101057091).

Author Contributions

STA and DT designed the study and performed the formal analysis. STA and DT analyzed and controlled the data. The manuscript was written by STA, ML, and DT. The experiments were performed by STA. The software was developed by STA. The statistical analyses were performed by STA and DT. The RSNA-RadioQA dataset was curated by STA, ML, and DT. The ExtendedQA dataset was curated by RS and DT. The human analysis was performed by LA. KB, RS, LA, DF, CK, JNK, SN, and DT provided clinical expertise. STA, ML, KB, JNK, and DT provided technical expertise. All authors read the manuscript, contributed to editing, and agreed to the submission of this paper.

Competing Interests

ML is employed by Generali Deutschland Services GmbH. JNK declares consulting services for Biotimus, France; Owkin, France; DoMore Diagnostics, Norway; Panakeia, UK; AstraZeneca, UK; Scailyte, Switzerland; Mindpeak, Germany; and MultiplexDx, Slovakia. Furthermore, he holds shares in StratifAI GmbH, Germany, has received a research grant by GSK, and has received honoraria by AstraZeneca, Bayer, Eisai, Janssen, MSD, BMS, Roche, Pfizer and Fresenius. DT holds shares in StratifAI GmbH and received honoraria for lectures by Bayer. The other authors do not have any competing interests to disclose.

References

1. Akinci D'Antonoli, T. *et al.* Large language models in radiology: fundamentals, applications, ethical considerations, risks, and future directions. *Diagnostic and Interventional Radiology* (2023) doi:10.4274/dir.2023.232417.
2. Tayebi Arasteh, S. *et al.* Large language models streamline automated machine learning for clinical studies. *Nat Commun* **15**, 1603 (2024).
3. Thirunavukarasu, A. J. *et al.* Large language models in medicine. *Nat Med* **29**, 1930–1940 (2023).
4. Clusmann, J. *et al.* The future landscape of large language models in medicine. *Commun Med* **3**, 141 (2023).
5. Adams, L. C. *et al.* Leveraging GPT-4 for Post Hoc Transformation of Free-text Radiology Reports into Structured Reporting: A Multilingual Feasibility Study. *Radiology* **307**, e230725 (2023).
6. Tayebi Arasteh, S. *et al.* The Treasure Trove Hidden in Plain Sight: The Utility of GPT-4 in Chest Radiograph Evaluation. *Radiology* **313**, e233441 (2024).
7. Fink, M. A. *et al.* Potential of ChatGPT and GPT-4 for Data Mining of Free-Text CT Reports on Lung Cancer. *Radiology* **308**, e231362 (2023).
8. Kottlors, J. *et al.* Feasibility of Differential Diagnosis Based on Imaging Patterns Using a Large Language Model. *Radiology* **308**, e231167 (2023).
9. Schmidt, R. A. *et al.* Generative Large Language Models for Detection of Speech Recognition Errors in Radiology Reports. *Radiology: Artificial Intelligence* **6**, e230205 (2024).
10. Alkaissi, H. & McFarlane, S. I. Artificial Hallucinations in ChatGPT: Implications in Scientific Writing. *Cureus* **15**, e35179 (2023).
11. Singhal, K. *et al.* Large language models encode clinical knowledge. *Nature* **620**, 172–180 (2023).
12. Ji, Z. *et al.* Survey of Hallucination in Natural Language Generation. *ACM Comput. Surv.* **55**, 1–38 (2023).
13. Christiano, P. F. *et al.* Deep Reinforcement Learning from Human Preferences. in *Advances in Neural Information Processing Systems* (eds. Guyon, I. *et al.*) vol. 30 (Curran Associates, Inc., 2017).
14. Wang, C. *et al.* Ethical Considerations of Using ChatGPT in Health Care. *J Med Internet Res* **25**, e48009 (2023).
15. Li, H. *et al.* Ethics of large language models in medicine and medical research. *Lancet Digit Health* **5**, e333–e335 (2023).
16. Truhn, D., Reis-Filho, J. S. & Kather, J. N. Large language models should be used as scientific reasoning engines, not knowledge databases. *Nat Med* **29**, 2983–2984 (2023).
17. Lewis, P. *et al.* Retrieval-Augmented Generation for Knowledge-Intensive NLP Tasks. in *Advances in Neural Information Processing Systems* (eds. Larochelle, H., Ranzato, M., Hadsell, R., Balcan, M. F. & Lin, H.) vol. 33 9459–9474 (Curran Associates, Inc., 2020).
18. Shuster, K., Poff, S., Chen, M., Kiela, D. & Weston, J. Retrieval Augmentation Reduces Hallucination in Conversation. Preprint at <http://arxiv.org/abs/2104.07567> (2021).
19. Zakka, C. *et al.* Almanac — Retrieval-Augmented Language Models for Clinical Medicine. *NEJM AI* **1**, (2024).
20. Xiong, G., Jin, Q., Lu, Z. & Zhang, A. Benchmarking Retrieval-Augmented Generation for Medicine. Preprint at <http://arxiv.org/abs/2402.13178> (2024).
21. Radiopaedia Australia Pty Ltd ACN 133 562 722. Radiopaedia.
22. Pal, A., Umapathi, L. K. & Sankarasubbu, M. MedMCQA : A Large-scale Multi-Subject Multi-Choice Dataset for Medical domain Question Answering. in *Proceedings of the Conference on Health, Inference, and Learning*, PMLR vol. 174 248–260 (2022).

23. Jin, Q., Dhingra, B., Liu, Z., Cohen, W. & Lu, X. PubMedQA: A Dataset for Biomedical Research Question Answering. in *Proceedings of the 2019 Conference on Empirical Methods in Natural Language Processing and the 9th International Joint Conference on Natural Language Processing (EMNLP-IJCNLP)* 2567–2577 (Association for Computational Linguistics, Hong Kong, China, 2019). doi:10.18653/v1/D19-1259.
24. Jacovi, A., Caciularu, A., Goldman, O. & Goldberg, Y. Stop Uploading Test Data in Plain Text: Practical Strategies for Mitigating Data Contamination by Evaluation Benchmarks. in *Proceedings of the 2023 Conference on Empirical Methods in Natural Language Processing* 5075–5084 (Association for Computational Linguistics, 2023).
25. Deep Mehta & Shubham H. Shinde Jr. Undifferentiated Embryonal Sarcoma. (2023) doi:10.1148/cases.20238698.
26. Wu, K. *et al.* How well do LLMs cite relevant medical references? An evaluation framework and analyses. Preprint at <http://arxiv.org/abs/2402.02008> (2024).
27. Reddy, S. Evaluating large language models for use in healthcare: A framework for translational value assessment. *Informatics in Medicine Unlocked* **41**, 101304 (2023).
28. Chiang, C.-H. & Lee, H. A Closer Look into Using Large Language Models for Automatic Evaluation. in *Findings of the Association for Computational Linguistics: EMNLP 2023* 8928–8942 (Association for Computational Linguistics, Singapore, 2023). doi:10.18653/v1/2023.findings-emnlp.599.
29. Han, T. *et al.* Comparative Analysis of Multimodal Large Language Model Performance on Clinical Vignette Questions. *JAMA* **331**, 1320 (2024).
30. Truhn, D. *et al.* Extracting structured information from unstructured histopathology reports using generative pre-trained transformer 4 (GPT -4). *The Journal of Pathology* **262**, 310–319 (2024).
31. Konietzschke, F. & Pauly, M. Bootstrapping and permuting paired t-test type statistics. *Stat Comput* **24**, 283–296 (2014).
32. Khader, F. *et al.* Artificial Intelligence for Clinical Interpretation of Bedside Chest Radiographs. *Radiology* **307**, e220510 (2022).
33. Wang, C. *et al.* Potential for GPT Technology to Optimize Future Clinical Decision-Making Using Retrieval-Augmented Generation. *Ann Biomed Eng* **52**, 1115–1118 (2024).
34. Kresevic, S. *et al.* Optimization of hepatological clinical guidelines interpretation by large language models: a retrieval augmented generation-based framework. *npj Digit. Med.* **7**, 102 (2024).
35. Gilbert, S., Kather, J. N. & Hogan, A. Augmented non-hallucinating large language models as medical information curators. *npj Digit. Med.* **7**, 100 (2024).
36. Yu, Y. *et al.* RankRAG: Unifying Context Ranking with Retrieval-Augmented Generation in LLMs. Preprint at <http://arxiv.org/abs/2407.02485> (2024).
37. Xi, Z. *et al.* The Rise and Potential of Large Language Model Based Agents: A Survey. Preprint at <http://arxiv.org/abs/2309.07864> (2023).
38. Ferber, D. *et al.* Development and validation of an autonomous artificial intelligence agent for clinical decision-making in oncology. *Nature Cancer* (2025) doi:<https://doi.org/10.1038/s43018-025-00991-6>.

Supplementary Information

Table S1: Accuracy results for individual specialties on the RSNA-RadioQA dataset. Mean accuracy, represented in percent, on RSNA-RadioQA with n=80 questions (details in **Appendix S1**).

Subspecialty	GPT-3.5-turbo		GPT-4		Mistral-7B		Mixtral-8x7B		Llama3-8B		Llama3-70B		Average	
	Radio RAG	No-RAG	Radio RAG	No-RAG	Radio RAG	No-RAG	Radio RAG	No-RAG	Radio RAG	No-RAG	Radio RAG	No-RAG	Radio RAG	No-RAG
Breast Imaging [n=10]	90	90	100	100	70	70	80	80	70	70	90	80	83	67
Cardiac [n=8]	50	50	62	62	38	50	62	50	38	50	50	12	50	33
Chest [n=13]	38	31	46	31	31	31	62	46	31	31	31	31	33	33
CT [n=28]	68	57	79	71	64	54	82	68	57	57	71	68	67	50
Emergency Radiology [n=6]	67	50	67	67	67	33	50	33	33	50	67	67	50	33
Gastrointestinal [n=12]	67	67	83	83	58	42	83	67	58	50	67	58	67	50
Genitourinary [n=8]	75	88	88	88	88	62	75	75	75	75	75	88	67	67
Head and Neck [n=9]	67	67	89	89	56	67	67	67	89	44	56	67	67	50
MRI [n=20]	95	90	90	85	65	70	85	75	60	75	80	80	67	67
Molecular Imaging [n=11]	55	55	64	64	55	55	64	64	55	64	55	45	50	50
Musculoskeletal [n=14]	93	93	93	86	64	71	79	64	64	71	86	86	67	67
Neuroradiology [n=11]	73	64	64	73	45	55	82	55	45	36	64	73	50	50
Nuclear Medicine [n=13]	62	62	69	69	54	54	69	69	62	62	54	46	50	50
Oncologic Imaging [n=16]	75	69	81	75	69	69	81	75	69	62	69	56	67	67
Pediatric [n=7]	43	14	43	43	29	14	57	14	29	14	43	29	33	17
Radiation Oncology [n=9]	89	89	89	78	78	78	89	89	78	56	78	89	83	67
Ultrasound [n=10]	90	90	90	90	60	70	80	70	70	70	90	70	67	67
Vascular Imaging [n=13]	77	54	69	69	46	46	69	69	46	62	62	54	50	50

Table S2: Overview of hallucination rates across LLMs. "Context relevant" refers to the percentage of cases where the retrieved articles and context were fully relevant to the question. Cases where the context was relevant but the response was still incorrect are classified as hallucinations. Results are presented for both the RSNA-RadioQA dataset (n=80 questions) and the ExtendedQA dataset (n=24 questions).

	RAG+GPT-3.5-turbo	RAG+GPT-4	RAG+Mistral-7B	RAG+Mixtral-8x7B	RAG+Llama 3-8B	RAG+Llama 3-70B
RSNA-RadioQA Dataset (n=80)						
Context relevant	72% (58/80)	72% (58/80)	72% (58/80)	72% (58/80)	72% (58/80)	72% (58/80)
Context relevant, response incorrect (hallucination)	10% (8/80)	6% (5/80)	25% (20/80)	9% (7/80)	22% (18/80)	14% (11/80)
Context irrelevant, response correct	10% (9/80)	12% (10/80)	7% (6/80)	12% (10/80)	9% (7/80)	10% (8/80)
Context irrelevant, response wrong	16% (13/80)	15% (12/80)	20% (16/80)	15% (12/80)	19% (15/80)	17% (14/80)
ExtendedQA Dataset (n=24)						
Context relevant	83% (20/24)	83% (20/24)	83% (20/24)	83% (20/24)	83% (20/24)	83% (20/24)
Context relevant, response incorrect (hallucination)	18% (4/24)	12% (3/24)	21% (5/24)	8% (2/24)	21% (5/24)	18% (4/24)
Context irrelevant, response correct	4% (1/24)	4% (1/24)	8% (2/24)	4% (1/24)	4% (1/24)	8% (2/24)
Context irrelevant, response wrong	12% (3/24)	12% (3/24)	8% (2/24)	12% (3/24)	12% (3/24)	8% (2/24)

Table S3: Answers of the RadioRAG-powered GPT-3.5-turbo to the first twenty questions of the RSNA-RadioQA dataset, together with the provided sources by the platform.

Question Identifier	LLM's (RadioRAG+GPT-3.5-turbo) Answer	Most Relevant Sources
RSNA-RadioQA-Q1	The most likely diagnosis is a benign fat-containing mass with rim calcifications.	https://radiopaedia.org/articles/breast-mass?lang=us , https://radiopaedia.org/articles/breast-imaging-reporting-and-data-system-bi-rads?lang=us
RSNA-RadioQA-Q2	The most likely diagnosis is phyllodes tumor of the breast.	https://radiopaedia.org/articles/breast-mri?lang=us , https://radiopaedia.org/articles/inflammatory-carcinoma-of-the-breast?lang=us
RSNA-RadioQA-Q3	Cat scratch disease lymphadenitis.	https://radiopaedia.org/articles/tuberculous-mastitis?lang=us , https://radiopaedia.org/articles/inflammatory-carcinoma-of-the-breast?lang=us , https://radiopaedia.org/articles/steatocystoma-multiplex-of-the-breast-1?lang=us
RSNA-RadioQA-Q4	The most likely diagnosis is invasive ductal carcinoma in both breasts.	https://radiopaedia.org/articles/bsbr-breast-imaging-classification?lang=us , https://radiopaedia.org/articles/breast-cancer-summary?lang=us , https://radiopaedia.org/articles/triple-receptor-negative-breast-cancer?lang=us
RSNA-RadioQA-Q5	The most likely diagnosis is bronchogenic carcinoma.	https://radiopaedia.org/articles/left-upper-lobe-collapse?lang=us , https://radiopaedia.org/articles/left-upper-lobe-collapse-in-the-exam?lang=us , https://radiopaedia.org/articles/bronchial-anthraco-fibrosis?lang=us
RSNA-RadioQA-Q6	The most likely diagnosis is organizing pneumonia.	https://radiopaedia.org/articles/acute-eosinophilic-pneumonia?lang=us , https://radiopaedia.org/articles/congestive-cardiac-failure?lang=us , https://radiopaedia.org/articles/rituximab-induced-interstitial-lung-disease-1?lang=us
RSNA-RadioQA-Q7	The most likely diagnosis is Tuberous Sclerosis Complex (TSC).	https://radiopaedia.org/articles/paediatric-cystic-renal-diseases?lang=us , https://radiopaedia.org/articles/tuberous-sclerosis?lang=us
RSNA-RadioQA-Q8	The most likely diagnosis is a patellar fracture.	https://radiopaedia.org/articles/osteoarthritis-of-the-hip?lang=us , https://radiopaedia.org/articles/osteoarthritis-of-the-knee?lang=us
RSNA-RadioQA-Q9	The most likely diagnosis is a post-traumatic aorto-left renal vein fistula.	https://radiopaedia.org/articles/aorto-left-renal-vein-fistula?lang=us , https://radiopaedia.org/articles/pelvic-lipomatosis?lang=us
RSNA-RadioQA-Q10	The most likely diagnosis is Hashimoto's thyroiditis.	https://radiopaedia.org/articles/steatocystoma-multiplex-of-the-breast-1?lang=us , https://radiopaedia.org/articles/acute-non-traumatic-abdominal-pain-in-pregnancy?lang=us , https://radiopaedia.org/articles/non-mass-enhancement-breast-mri?lang=us
RSNA-RadioQA-Q11	The most likely diagnosis is sarcoidosis.	https://radiopaedia.org/articles/dacryoadenitis?lang=us , https://radiopaedia.org/articles/idiopathic-orbital-inflammation?lang=us
RSNA-RadioQA-Q12	The most likely diagnosis is epidural angioliopoma.	https://radiopaedia.org/articles/cauda-equina-syndrome?lang=us , https://radiopaedia.org/articles/extradural-spinal-cavernous-malformation?lang=us , https://radiopaedia.org/articles/low-back-pain?lang=us
RSNA-RadioQA-Q13	The most likely diagnosis is a femoral diaphyseal stress injury.	https://radiopaedia.org/articles/femoral-diaphyseal-stress-injury?lang=us , https://radiopaedia.org/articles/osteoarthritis-of-the-hip?lang=us
RSNA-RadioQA-Q14	The most likely diagnosis is Kienbock's disease.	https://radiopaedia.org/articles/ulnar-impaction-syndrome?lang=us , https://radiopaedia.org/articles/kienbock-disease-2?lang=us
RSNA-RadioQA-Q15	LR-1 - benign simple cyst.	https://radiopaedia.org/articles/li-rads-us-surveillance?lang=us , https://radiopaedia.org/articles/ctmri-li-rads?lang=us
RSNA-RadioQA-Q16	The most likely diagnosis is Tenosynovial giant cell tumor (TGCT).	https://radiopaedia.org/articles/soft-tissue-mass?lang=us , https://radiopaedia.org/articles/tenosynovial-giant-cell-tumour-2?lang=us , https://radiopaedia.org/articles/flexor-pronator-mass-injury?lang=us
RSNA-RadioQA-Q17	The most likely diagnosis is alveolar soft part sarcoma (ASPS).	https://radiopaedia.org/articles/alveolar-soft-part-sarcoma-2?lang=us , https://radiopaedia.org/articles/stromal-tumour-of-uncertain-malignant-potential?lang=us
RSNA-RadioQA-Q18	The most likely diagnosis is an old avulsion fracture of the inferior pole of the patella with remodeling.	https://radiopaedia.org/articles/anterior-cruciate-ligament-avulsion-fracture?lang=us , https://radiopaedia.org/articles/tibial-tuberosity-avulsion-fracture?lang=us , https://radiopaedia.org/articles/paediatric-knee-radiograph-an-approach?lang=us
RSNA-RadioQA-Q19	The most likely diagnosis is a benign complicated cyst in the right breast.	https://radiopaedia.org/articles/mature-cystic-ovarian-teratoma-1?lang=us , https://radiopaedia.org/articles/nodular-pulmonary-amyloidosis?lang=us , https://radiopaedia.org/articles/mammary-duct-ectasia?lang=us
RSNA-RadioQA-Q20	The most likely diagnosis is a retroperitoneal teratoma.	https://radiopaedia.org/articles/peritoneal-inclusion-cyst?lang=us

Table S4: Answers of the conventional GPT-3.5-turbo to the first thirty questions of RSNA-RadioQA dataset. For the original questions and their ground truth answers of the RSNA-RadioQA dataset, refer to **Appendix S1**.

Question Identifier	LLM's (GPT-3.5-turbo) Answer
RSNA-RadioQA-Q1	The most likely diagnosis is a benign breast lesion, such as a lipoma or fibroadenoma, with associated calcifications.
RSNA-RadioQA-Q2	The most likely diagnosis is desmoid tumor (also known as aggressive fibromatosis).
RSNA-RadioQA-Q3	The most likely diagnosis is Cat Scratch Disease (CSD) with suppurative granulomatous lymphadenitis.
RSNA-RadioQA-Q4	The most likely diagnosis is bilateral invasive ductal carcinoma of the breast, ER positive, PR positive, and HER2 negative, with no lymph node involvement.
RSNA-RadioQA-Q5	The most likely diagnosis is pulmonary rhabdomyosarcoma.
RSNA-RadioQA-Q6	The most likely diagnosis is severe COVID-19 pneumonia.
RSNA-RadioQA-Q7	The most likely diagnosis is pulmonary lymphangioleiomyomatosis (LAM), a characteristic manifestation of Tuberous Sclerosis Complex (TSC).
RSNA-RadioQA-Q8	The most likely diagnosis is a patellar fracture.
RSNA-RadioQA-Q9	The most likely diagnosis is diverticulitis with associated pericolonic inflammation and phlegmon formation.
RSNA-RadioQA-Q10	The most likely diagnosis is Hashimoto's thyroiditis.
RSNA-RadioQA-Q11	The most likely diagnosis is orbital sarcoidosis.
RSNA-RadioQA-Q12	The most likely diagnosis is epidural spinal hemangioma.
RSNA-RadioQA-Q13	The most likely diagnosis is a stress fracture of the left femoral neck.
RSNA-RadioQA-Q14	The most likely diagnosis is Kienböck's disease.
RSNA-RadioQA-Q15	The most likely diagnosis is a benign simple cyst of the liver.
RSNA-RadioQA-Q16	The most likely diagnosis is Giant Cell Tumor of Tendon Sheath (GCTTS).
RSNA-RadioQA-Q17	The most likely diagnosis is Alveolar soft part sarcoma (ASPS).
RSNA-RadioQA-Q18	The most likely diagnosis is patellar tendon avulsion fracture.
RSNA-RadioQA-Q19	The most likely diagnosis is benign complicated cysts, given the resolution of the mass with aspiration and the benign nature of the identified cysts on imaging.
RSNA-RadioQA-Q20	The most likely diagnosis is a retroperitoneal teratoma.
RSNA-RadioQA-Q21	The most likely diagnosis is solitary fibrous tumor (SFT) of the thigh.
RSNA-RadioQA-Q22	The most likely diagnosis is a renal artery aneurysm.
RSNA-RadioQA-Q23	The most likely diagnosis is popliteal artery entrapment syndrome.
RSNA-RadioQA-Q24	The most likely diagnosis is osteosarcoma.
RSNA-RadioQA-Q25	The most likely diagnosis is pulmonary embolism.
RSNA-RadioQA-Q26	The most likely diagnosis is recurrent pericarditis, possibly related to systemic lupus erythematosus.
RSNA-RadioQA-Q27	The most likely diagnosis is gastroschisis with associated omphalocele and cleft lip/palate.
RSNA-RadioQA-Q28	The most likely diagnosis is adenocarcinoma of the ileocecal region.
RSNA-RadioQA-Q29	Biliary atresia.
RSNA-RadioQA-Q30	The most likely diagnosis is an incarcerated inguinal hernia with an acutely inflamed, herniated appendix, known as Amyand's hernia.

Appendix S1

The Radiological Society of North America Case Collection adapted to RadioRAG pipeline question answering (RSNA-RadioQA) dataset, consists of 80 expert-curated questions. The complete dataset with all the questions and their corresponding answers is as follows.

Question Identifier: RSNA-RadioQA-Q1

DOI of the Original Case: 10.1148/cases.20227914.

Authors of the Original Case: K. Elzinga, R. Woods.

Title of the Original Case: BI-RADS 2: Rim Calcifications.

Publication Date of the Original Case: 10/10/2022.

Supspecialties: Breast Imaging.

Copyright © Radiological Society of North America, Inc. (RSNA), All Rights Reserved

Question Identifier: RSNA-RadioQA-Q2

DOI of the Original Case: 10.1148/cases.20227478.

Authors of the Original Case: A. Aripoli, P. Iglar, E. Friedman.

Title of the Original Case: Breast Fibromatosis.

Publication Date of the Original Case: 8/8/2022.

Supspecialties: Breast Imaging.

Copyright © Radiological Society of North America, Inc. (RSNA), All Rights Reserved

Question Identifier: RSNA-RadioQA-Q3

DOI of the Original Case: 10.1148/cases.20239154.

Authors of the Original Case: C. Ayeni, L. Misbach, M. Quintana, P. Slanetz.

Title of the Original Case: Cat-Scratch Disease.

Publication Date of the Original Case: 4/25/2023.

Supspecialties: Breast Imaging, Ultrasound.

Copyright © Radiological Society of North America, Inc. (RSNA), All Rights Reserved

Question Identifier: RSNA-RadioQA-Q4

DOI of the Original Case: 10.1148/cases.20238930.

Authors of the Original Case: L. Shah, T. Kuritza, S. Benjamin, R. Ganesh.

Title of the Original Case: Bilateral Synchronous Invasive Ductal Carcinoma in a Male.

Publication Date of the Original Case: 3/17/2023.

Supspecialties: Breast Imaging, Ultrasound.

Copyright © Radiological Society of North America, Inc. (RSNA), All Rights Reserved

Question Identifier: RSNA-RadioQA-Q5

DOI of the Original Case: 10.1148/cases.20239212.

Authors of the Original Case: C. Walker, S. Gerrie, M. Aquino.

Title of the Original Case: Pleuropulmonary Blastoma.

Publication Date of the Original Case: 5/19/2023.

Supspecialties: Chest, Pediatric.

Copyright © Radiological Society of North America, Inc. (RSNA), All Rights Reserved

Question Identifier: RSNA-RadioQA-Q6

DOI of the Original Case: 10.1148/cases.20238747.

Authors of the Original Case: J. Daniel, S. Ayad Al-Katib.

Title of the Original Case: Post-COVID Interstitial Lung Disease.

Publication Date of the Original Case: 3/3/2023.

Supspecialties: Computed Tomography, Chest.

Copyright © Radiological Society of North America, Inc. (RSNA), All Rights Reserved

Question Identifier: RSNA-RadioQA-Q7

DOI of the Original Case: 10.1148/cases.20238883.

Authors of the Original Case: N. Raval, R. Jha, P. Bergquist, N. Jain.

Title of the Original Case: Multifocal Micronodular Pneumocyte Hyperplasia.
Publication Date of the Original Case: 2/6/2023.
Supspecialties: Computed Tomography, Chest.
Copyright © Radiological Society of North America, Inc. (RSNA), All Rights Reserved

Question Identifier: RSNA-RADIOQA-Q8

DOI of the Original Case: 10.1148/cases.20227185.
Authors of the Original Case: B. Guthridge, B. Fink.
Title of the Original Case: Vertical Patellar Fracture.
Publication Date of the Original Case: 12/1/2022.
Supspecialties: Emergency Radiology, Musculoskeletal.
Copyright © Radiological Society of North America, Inc. (RSNA), All Rights Reserved

Question Identifier: RSNA-RadioQA-Q9

DOI of the Original Case: 10.1148/cases.20226345.
Authors of the Original Case: B. Tallman, R. Jarman.
Title of the Original Case: Epiploic Appendagitis.
Publication Date of the Original Case: 1/31/2022.
Supspecialties: Gastrointestinal, Emergency Radiology, Computed Tomography.
Copyright © Radiological Society of North America, Inc. (RSNA), All Rights Reserved

Question Identifier: RSNA-RadioQA-Q10

DOI of the Original Case: 10.1148/cases.20224821.
Authors of the Original Case: Q. Li, J. Wang, D. Gao, T. Pierce.
Title of the Original Case: Hashimoto's thyroiditis.
Publication Date of the Original Case: 4/4/2022.
Supspecialties: Ultrasound, Head and Neck.
Copyright © Radiological Society of North America, Inc. (RSNA), All Rights Reserved

Question Identifier: RSNA-RadioQA-Q11

DOI of the Original Case: 10.1148/cases.20238331.
Authors of the Original Case: A. Kumar, D. Gewolb, A. Narayan.
Title of the Original Case: Orbital Sarcoidosis.
Publication Date of the Original Case: 2/15/2023.
Supspecialties: Head and Neck, Neuroradiology.
Copyright © Radiological Society of North America, Inc. (RSNA), All Rights Reserved

Question Identifier: RSNA-RadioQA-Q12

DOI of the Original Case: 10.1148/cases.20224694.
Authors of the Original Case: L. Chiu, J. Yoon
Title of the Original Case: Spinal Angiolipoma.
Publication Date of the Original Case: 11/10/2022.
Supspecialties: Neuroradiology, Magnetic Resonance Imaging.
Copyright © Radiological Society of North America, Inc. (RSNA), All Rights Reserved

Question Identifier: RSNA-RadioQA-Q13

DOI of the Original Case: 10.1148/cases.20227653.
Authors of the Original Case: G. Rahmani.
Title of the Original Case: Femoral neck stress fracture.
Publication Date of the Original Case: 12/8/2022.
Supspecialties: Magnetic Resonance Imaging, Musculoskeletal.
Copyright © Radiological Society of North America, Inc. (RSNA), All Rights Reserved

Question Identifier: RSNA-RadioQA-Q14

DOI of the Original Case: 10.1148/cases.20227689.
Authors of the Original Case: T. Schermann, R. Potenza, T. DenOtter.
Title of the Original Case: Kienbock Disease.
Publication Date of the Original Case: 12/19/2022.
Supspecialties: Musculoskeletal, Magnetic Resonance Imaging.
Copyright © Radiological Society of North America, Inc. (RSNA), All Rights Reserved

Question Identifier: RSNA-RadioQA-Q15

DOI of the Original Case: 10.1148/cases.20238060.
Authors of the Original Case: A. Alkhudari, A. Gibson, J. Lee, A. Sobieh.
Title of the Original Case: LI-RADS 1.
Publication Date of the Original Case: 3/6/2023.
Supspecialties: Gastrointestinal, Magnetic Resonance Imaging.
Copyright © Radiological Society of North America, Inc. (RSNA), All Rights Reserved

Question Identifier: RSNA-RadioQA-Q16

DOI of the Original Case: 10.1148/cases.20238375.
Authors of the Original Case: J. Paek, R. Rozzi, J. Judge.
Title of the Original Case: Tenosynovial Giant Cell Tumor of the Finger.
Publication Date of the Original Case: 3/17/2023.
Supspecialties: Musculoskeletal, Magnetic Resonance Imaging.
Copyright © Radiological Society of North America, Inc. (RSNA), All Rights Reserved

Question Identifier: RSNA-RadioQA-Q17

DOI of the Original Case: 10.1148/cases.20237558.
Authors of the Original Case: B. Franz, P. Patel, C. Scher.
Title of the Original Case: Alveolar Soft Part Sarcoma.
Publication Date of the Original Case: 4/18/2023.
Supspecialties: Musculoskeletal, Magnetic Resonance Imaging.
Copyright © Radiological Society of North America, Inc. (RSNA), All Rights Reserved

Question Identifier: RSNA-RadioQA-Q18

DOI of the Original Case: 10.1148/cases.20238620.
Authors of the Original Case: R. Iyer, M. Kumaravel.
Title of the Original Case: Patellar tendon tear.
Publication Date of the Original Case: 5/12/2023.
Supspecialties: Musculoskeletal, Magnetic Resonance Imaging.
Copyright © Radiological Society of North America, Inc. (RSNA), All Rights Reserved

Question Identifier: RSNA-RadioQA-Q19

DOI of the Original Case: 10.1148/cases.20225780.
Authors of the Original Case: N. Vu, R. Woods.
Title of the Original Case: Complicated Breast Cyst.
Publication Date of the Original Case: 2/24/2022.
Supspecialties: Magnetic Resonance Imaging, Breast Imaging.
Copyright © Radiological Society of North America, Inc. (RSNA), All Rights Reserved

Question Identifier: RSNA-RadioQA-Q20

DOI of the Original Case: 10.1148/cases.20238293.
Authors of the Original Case: S. Carter, F. Flaherty.
Title of the Original Case: Primary Retroperitoneal Mature Cystic Teratoma.
Publication Date of the Original Case: 3/27/2023.
Supspecialties: Magnetic Resonance Imaging, Computed Tomography.
Copyright © Radiological Society of North America, Inc. (RSNA), All Rights Reserved

Question Identifier: RSNA-RadioQA-Q21

DOI of the Original Case: 10.1148/cases.20237602.
Authors of the Original Case: L. Verst, D. Constantino, M. Chalian.
Title of the Original Case: Solitary Fibrous Tumor.
Publication Date of the Original Case: 2/6/2023.
Supspecialties: Musculoskeletal, Magnetic Resonance Imaging, Ultrasound.
Copyright © Radiological Society of North America, Inc. (RSNA), All Rights Reserved

Question Identifier: RSNA-RadioQA-Q22

DOI of the Original Case: 10.1148/cases.20238276.
Authors of the Original Case: S. Goddard, A. Annamalai, C. Chamberlin, B. Triche.
Title of the Original Case: Renal Arteriovenous Malformation.
Publication Date of the Original Case: 6/8/2023.
Supspecialties: Vascular Imaging, Interventional Radiology, Computed Tomography, Genitourinary.
Copyright © Radiological Society of North America, Inc. (RSNA), All Rights Reserved

Question Identifier: RSNA-RadioQA-Q23

DOI of the Original Case: 10.1148/cases.20238491.

Authors of the Original Case: E. Berger, M. MacDonald.

Title of the Original Case: Popliteal Artery Entrapment Syndrome with Thrombosis.

Publication Date of the Original Case: 6/8/2023.

Supspecialties: Ultrasound, Computed Tomography, Vascular Imaging, Musculoskeletal.

Copyright © Radiological Society of North America, Inc. (RSNA), All Rights Reserved

Question Identifier: RSNA-RadioQA-Q24

DOI of the Original Case: 10.1148/cases.20238762.

Authors of the Original Case: N. LeCrone, A. Goggins, Y. Qiao, A. Salem.

Title of the Original Case: Conventional Osteosarcoma.

Publication Date of the Original Case: 6/7/2023.

Supspecialties: Musculoskeletal.

Copyright © Radiological Society of North America, Inc. (RSNA), All Rights Reserved

Question Identifier: RSNA-RadioQA-Q25

DOI of the Original Case: 10.1148/cases.20239055.

Authors of the Original Case: F. Lo, S. Robert, G. Brahm.

Title of the Original Case: Epipericardial Fat Necrosis.

Publication Date of the Original Case: 3/3/2023.

Supspecialties: Computed Tomography, Cardiac, Emergency Radiology, Chest.

Copyright © Radiological Society of North America, Inc. (RSNA), All Rights Reserved

Question Identifier: RSNA-RadioQA-Q26

DOI of the Original Case: 10.1148/cases.20226457.

Authors of the Original Case: A. Canan, N. Cabrera.

Title of the Original Case: Cardiac tamponade.

Publication Date of the Original Case: 1/16/2022.

Supspecialties: Magnetic Resonance Imaging, Computed Tomography, Cardiac.

Copyright © Radiological Society of North America, Inc. (RSNA), All Rights Reserved

Question Identifier: RSNA-RadioQA-Q27

DOI of the Original Case: 10.1148/cases.20239046.

Authors of the Original Case: V. Krishnan, S. Jaganathan, K. Schmitz, M. Renno.

Title of the Original Case: Pentalogy of Cantrell.

Publication Date of the Original Case: 3/3/2023.

Supspecialties: Cardiac, Gastrointestinal, Computed Tomography, Pediatric.

Copyright © Radiological Society of North America, Inc. (RSNA), All Rights Reserved

Question Identifier: RSNA-RadioQA-Q28

DOI of the Original Case: 10.1148/cases.20227592.

Authors of the Original Case: Y. Park, O. Kalinkin.

Title of the Original Case: Small Bowel Carcinoid Tumor.

Publication Date of the Original Case: 7/11/2022.

Supspecialties: Gastrointestinal, Computed Tomography.

Copyright © Radiological Society of North America, Inc. (RSNA), All Rights Reserved

Question Identifier: RSNA-RadioQA-Q29

DOI of the Original Case: 10.1148/cases.20228374.

Authors of the Original Case: K. Banks.

Title of the Original Case: Biliary Atresia.

Publication Date of the Original Case: 10/20/2022.

Supspecialties: Nuclear Medicine, Gastrointestinal.

Copyright © Radiological Society of North America, Inc. (RSNA), All Rights Reserved

Question Identifier: RSNA-RadioQA-Q30

DOI of the Original Case: 10.1148/cases.20227840.

Authors of the Original Case: C. Qian, N. Parikh, J. Oh, J. Amorosa.

Title of the Original Case: Amyand Hernia with Appendicitis.

Publication Date of the Original Case: 11/2/2022.

Supspecialties: Genitourinary, Gastrointestinal, Computed Tomography.

Question Identifier: RSNA-RadioQA-Q31

DOI of the Original Case: 10.1148/cases.20225796.

Authors of the Original Case: A. Bamashmos, K. Elfatairy, R. Hegde, O. Awan.

Title of the Original Case: Cervical spine gout.

Publication Date of the Original Case: 1/14/2022.

Supspecialties: Computed Tomography, Musculoskeletal.

Copyright © Radiological Society of North America, Inc. (RSNA), All Rights Reserved

Question Identifier: RSNA-RadioQA-Q32

DOI of the Original Case: 10.1148/cases.20227086.

Authors of the Original Case: J. Benjamin, H. Son.

Title of the Original Case: Septic Embolism.

Publication Date of the Original Case: 4/15/2022.

Supspecialties: Chest, Computed Tomography.

Copyright © Radiological Society of North America, Inc. (RSNA), All Rights Reserved

Question Identifier: RSNA-RadioQA-Q33

DOI of the Original Case: 10.1148/cases.20227539.

Authors of the Original Case: A. Shah, O. Shah, T. Shera, S. Shabir.

Title of the Original Case: Erdheim-Chester disease.

Publication Date of the Original Case: 9/21/2022.

Supspecialties: Computed Tomography, Chest.

Copyright © Radiological Society of North America, Inc. (RSNA), All Rights Reserved

Question Identifier: RSNA-RadioQA-Q34

DOI of the Original Case: 10.1148/cases.20226333.

Authors of the Original Case: Z. Timmerman, M. Carrillo, B. Shah.

Title of the Original Case: Male invasive Ductal Carcinoma.

Publication Date of the Original Case: 1/19/2022.

Supspecialties: Ultrasound, Breast Imaging, Oncologic Imaging.

Copyright © Radiological Society of North America, Inc. (RSNA), All Rights Reserved

Question Identifier: RSNA-RadioQA-Q35

DOI of the Original Case: 10.1148/cases.20239100.

Authors of the Original Case: J. Eichhorn, M. Fox.

Title of the Original Case: FDG -avid axillary lymphadenopathy.

Publication Date of the Original Case: 2/15/2023.

Supspecialties: Nuclear Medicine, Oncologic Imaging, Molecular Imaging, Chest.

Copyright © Radiological Society of North America, Inc. (RSNA), All Rights Reserved

Question Identifier: RSNA-RadioQA-Q36

DOI of the Original Case: 10.1148/cases.20239042.

Authors of the Original Case: J. Eichhorn, N. Phelan, J. Gilstrap.

Title of the Original Case: Polyostotic Paget Disease.

Publication Date of the Original Case: 3/3/2023.

Supspecialties: Musculoskeletal, Molecular Imaging, Breast Imaging, Nuclear Medicine, Oncologic Imaging.

Copyright © Radiological Society of North America, Inc. (RSNA), All Rights Reserved

Question Identifier: RSNA-RadioQA-Q37

DOI of the Original Case: 10.1148/cases.20238698.

Authors of the Original Case: D. Mehta, S. Shinde.

Title of the Original Case: Undifferentiated Embryonal Sarcoma.

Publication Date of the Original Case: 1/17/2023.

Supspecialties: Pediatric, Oncologic Imaging.

Copyright © Radiological Society of North America, Inc. (RSNA), All Rights Reserved

Question Identifier: RSNA-RadioQA-Q38

DOI of the Original Case: 10.1148/cases.20228072.

Authors of the Original Case: I. Buren, A. Fung.

Title of the Original Case: LI-RADS TIV.

Publication Date of the Original Case: 10/24/2022.

Supspecialties: Computed Tomography, Oncologic Imaging, Magnetic Resonance Imaging, Gastrointestinal, Radiation Oncology.

Copyright © Radiological Society of North America, Inc. (RSNA), All Rights Reserved

Question Identifier: RSNA-RadioQA-Q39

DOI of the Original Case: 10.1148/cases.20223617.

Authors of the Original Case: M. Roda, P. McGeorge, J. Rangunwala, T. Banta.

Title of the Original Case: Acute Radiation Enteropathy.

Publication Date of the Original Case: 3/23/2021.

Supspecialties: Computed Tomography, Radiation Oncology, Oncologic Imaging, Gastrointestinal.

Copyright © Radiological Society of North America, Inc. (RSNA), All Rights Reserved

Question Identifier: RSNA-RadioQA-Q40

DOI of the Original Case: 10.1148/cases.20221945.

Authors of the Original Case: K. Nutter, J. Chaudry, D. Kennedy, R. Morris.

Title of the Original Case: Bisphosphonate Induced Mandibular Osteonecrosis.

Publication Date of the Original Case: 6/16/2020.

Supspecialties: Musculoskeletal, Radiation Oncology, Head and Neck, Nuclear Medicine, Oncologic Imaging.

Copyright © Radiological Society of North America, Inc. (RSNA), All Rights Reserved

Question Identifier: RSNA-RadioQA-Q41

DOI of the Original Case: 10.1148/cases.20221974.

Authors of the Original Case: R. Savjani, Y. Yang, A. Kishan, R. Morris.

Title of the Original Case: Hydrogel infiltration into rectal wall.

Publication Date of the Original Case: 10/14/2020.

Supspecialties: Computed Tomography, Oncologic Imaging, Radiation Oncology, Gastrointestinal, Genitourinary, Magnetic Resonance Imaging.

Copyright © Radiological Society of North America, Inc. (RSNA), All Rights Reserved

Question Identifier: RSNA-RadioQA-Q42

DOI of the Original Case: 10.1148/cases.2022988.

Authors of the Original Case: N. Zakhari, Y. Yang, A. Kishan, R. Morris.

Title of the Original Case: Multifocal Glioblastoma.

Publication Date of the Original Case: 5/4/2020.

Supspecialties: Radiation Oncology, Neuroradiology, Magnetic Resonance Imaging, Computed Tomography.

Copyright © Radiological Society of North America, Inc. (RSNA), All Rights Reserved

Question Identifier: RSNA-RadioQA-Q43

DOI of the Original Case: 10.1148/cases.20238786.

Authors of the Original Case: P. Gonzalez, J. Diaz, G. Schiappacasse, P. Rios.

Title of the Original Case: Endometriosis-associated neuropathy.

Publication Date of the Original Case: 3/16/2023.

Supspecialties: Emergency Radiology, Genitourinary, Magnetic Resonance Imaging, General/Other, Musculoskeletal, Obstetrics/Gynecology.

Copyright © Radiological Society of North America, Inc. (RSNA), All Rights Reserved

Question Identifier: RSNA-RadioQA-Q45

DOI of the Original Case: 10.1148/cases.20221612.

Authors of the Original Case: R. McCallum, N. Mallak, A. Camacho.

Title of the Original Case: Ventriculoperitoneal Shunt Distal Limb Obstruction.

Publication Date of the Original Case: 1/7/2021.

Supspecialties: Molecular Imaging, Neuroradiology, Nuclear Medicine.

Copyright © Radiological Society of North America, Inc. (RSNA), All Rights Reserved

Question Identifier: RSNA-RadioQA-Q46

DOI of the Original Case: 10.1148/cases.20225551.

Authors of the Original Case: T. Dittmer, W. Rieter, S. Elojeimy.

Title of the Original Case: Carotid Body Paraganglioma.

Publication Date of the Original Case: 12/6/2021.

Supspecialties: Nuclear Medicine, Head and Neck, Molecular Imaging.

Copyright © Radiological Society of North America, Inc. (RSNA), All Rights Reserved

Question Identifier: RSNA-RadioQA-Q47

DOI of the Original Case: 10.1148/cases.20226289.

Authors of the Original Case: O. Schoeck, H. Tran, S. Elojeimy.

Title of the Original Case: Sister Mary Joseph Nodule.

Publication Date of the Original Case: 12/9/2021.

Supspecialties: Oncologic Imaging, Computed Tomography, Nuclear Medicine, Genitourinary, Molecular Imaging.

Copyright © Radiological Society of North America, Inc. (RSNA), All Rights Reserved

Question Identifier: RSNA-RadioQA-Q48

DOI of the Original Case: 10.1148/cases.20223739.

Authors of the Original Case: F. Siddiqui, A. Chauhan, A. Khurana.

Title of the Original Case: Pseudoprogession with Immunotherapy Treatment.

Publication Date of the Original Case: 2/4/2021.

Supspecialties: Oncologic Imaging, Molecular Imaging, Head and Neck, Nuclear Medicine.

Copyright © Radiological Society of North America, Inc. (RSNA), All Rights Reserved

Question Identifier: RSNA-RadioQA-Q49

DOI of the Original Case: 10.1148/cases.20222626.

Authors of the Original Case: D. Bitonte, S. Snodgrass.

Title of the Original Case: Hibernating Myocardium.

Publication Date of the Original Case: 11/3/2020.

Supspecialties: Nuclear Medicine, Magnetic Resonance Imaging, Molecular Imaging, Cardiac.

Copyright © Radiological Society of North America, Inc. (RSNA), All Rights Reserved

Question Identifier: RSNA-RadioQA-Q50

DOI of the Original Case: 10.1148/cases.20221744.

Authors of the Original Case: M. Yang, R. Shrestha, J. Zhang, M. Roarke.

Title of the Original Case: "Cold" Sentinel Lymph Node in Cutaneous Melanoma.

Publication Date of the Original Case: 6/5/2020.

Supspecialties: Oncologic Imaging, Molecular Imaging, Nuclear Medicine, General/Other.

Copyright © Radiological Society of North America, Inc. (RSNA), All Rights Reserved

Question Identifier: RSNA-RadioQA-Q51

DOI of the Original Case: 10.1148/cases.20221826.

Authors of the Original Case: K. Addae-Mensah, M. Tafoya, S. Elojeimy.

Title of the Original Case: Groove pancreatitis.

Publication Date of the Original Case: 5/7/2020.

Supspecialties: Nuclear Medicine, Molecular Imaging, Gastrointestinal, Emergency Radiology, Computed Tomography.

Copyright © Radiological Society of North America, Inc. (RSNA), All Rights Reserved

Question Identifier: RSNA-RadioQA-Q52

DOI of the Original Case: 10.1148/cases.20221848.

Authors of the Original Case: S. Elojeimy, S. Behnia.

Title of the Original Case: Elastofibroma dorsi.

Publication Date of the Original Case: 4/10/2020.

Supspecialties: Molecular Imaging, Oncologic Imaging, Musculoskeletal, Nuclear Medicine.

Copyright © Radiological Society of North America, Inc. (RSNA), All Rights Reserved

Question Identifier: RSNA-RadioQA-Q53

DOI of the Original Case: 10.1148/cases.20221602.

Authors of the Original Case: W. Crawford, C. Walker.

Title of the Original Case: Cardiac myxoma.

Publication Date of the Original Case: 4/8/2020.

Supspecialties: General/Other, Oncologic Imaging, Ultrasound, Vascular Imaging, Chest, Magnetic Resonance Imaging, Cardiac.

Copyright © Radiological Society of North America, Inc. (RSNA), All Rights Reserved

Question Identifier: RSNA-RadioQA-Q54

DOI of the Original Case: 10.1148/cases.20222739.

Authors of the Original Case: L. Raspante, T. Foureaux, E. Ayub, C. Silva.

Title of the Original Case: Neonatal tuberous sclerosis.

Publication Date of the Original Case: 11/4/2020.
Supspecialties: Pediatric, Cardiac, Magnetic Resonance Imaging, Ultrasound, Obstetrics/Gynecology, Neuroradiology.
Copyright © Radiological Society of North America, Inc. (RSNA), All Rights Reserved

Question Identifier: RSNA-RadioQA-Q55

DOI of the Original Case: 10.1148/cases.20223038.
Authors of the Original Case: E. Barkovich, N. Khati.
Title of the Original Case: Subclavian Stenosis with Pre-Steal.
Publication Date of the Original Case: 9/8/2021.
Supspecialties: Vascular Imaging, Ultrasound.
Copyright © Radiological Society of North America, Inc. (RSNA), All Rights Reserved

Question Identifier: RSNA-RadioQA-Q56

DOI of the Original Case: 10.1148/cases.20225859.
Authors of the Original Case: J. Madsen, C. Cooley, C. Dumas.
Title of the Original Case: Aortoiliac Occlusive Disease.
Publication Date of the Original Case: 9/29/2021.
Supspecialties: Computed Tomography, Vascular Imaging.
Copyright © Radiological Society of North America, Inc. (RSNA), All Rights Reserved

Question Identifier: RSNA-RadioQA-Q57

DOI of the Original Case: 10.1148/cases.20224513.
Authors of the Original Case: D. Bittles, A. Gunn.
Title of the Original Case: Post-Traumatic Arteriovenous Fistula.
Publication Date of the Original Case: 4/21/2021.
Supspecialties: Interventional Radiology, Vascular Imaging.
Copyright © Radiological Society of North America, Inc. (RSNA), All Rights Reserved

Question Identifier: RSNA-RadioQA-Q58

DOI of the Original Case: 10.1148/cases.20224581.
Authors of the Original Case: J. Liu, V. Gorolay.
Title of the Original Case: Acute Aortoiliac Occlusion.
Publication Date of the Original Case: 3/15/2021.
Supspecialties: Computed Tomography, Vascular Imaging.
Copyright © Radiological Society of North America, Inc. (RSNA), All Rights Reserved

Question Identifier: RSNA-RadioQA-Q59

DOI of the Original Case: 10.1148/cases.20222067.
Authors of the Original Case: J. Shen, R. Lim.
Title of the Original Case: Pulmonary arteriovenous malformation.
Publication Date of the Original Case: 6/16/2020.
Supspecialties: Cardiac, Vascular Imaging, Chest.
Copyright © Radiological Society of North America, Inc. (RSNA), All Rights Reserved

Question Identifier: RSNA-RadioQA-Q60

DOI of the Original Case: 10.1148/cases.20222080.
Authors of the Original Case: J. Shen, J. Tse, R. Lim.
Title of the Original Case: Pulmonary Embolism with Right Heart Strain.
Publication Date of the Original Case: 5/15/2020.
Supspecialties: Cardiac, Chest, Vascular Imaging.
Copyright © Radiological Society of North America, Inc. (RSNA), All Rights Reserved

Question Identifier: RSNA-RadioQA-Q61

DOI of the Original Case: 10.1148/cases.20223188.
Authors of the Original Case: O. Yusufzai, P. Patel.
Title of the Original Case: Thoracic Aortic Pseudoaneurysm.
Publication Date of the Original Case: 4/6/2021.
Supspecialties: Chest, Vascular Imaging, Computed Tomography.
Copyright © Radiological Society of North America, Inc. (RSNA), All Rights Reserved

Question Identifier: RSNA-RadioQA-Q62

DOI of the Original Case: 10.1148/cases.20223594.
Authors of the Original Case: A. Ritchey, J. Kucera.
Title of the Original Case: Takayasu Arteritis.
Publication Date of the Original Case: 12/7/2020.
Supspecialties: Interventional Radiology, Pediatric, Vascular Imaging.
Copyright © Radiological Society of North America, Inc. (RSNA), All Rights Reserved

Question Identifier: RSNA-RadioQA-Q63

DOI of the Original Case: 10.1148/cases.20223946.
Authors of the Original Case: R. Davidyan, S. Singh.
Title of the Original Case: Duplicated Inferior Vena Cava.
Publication Date of the Original Case: 9/15/2021.
Supspecialties: Computed Tomography, Vascular Imaging, Interventional Radiology.
Copyright © Radiological Society of North America, Inc. (RSNA), All Rights Reserved

Question Identifier: RSNA-RadioQA-Q64

DOI of the Original Case: 10.1148/cases.20224487.
Authors of the Original Case: S. Srinivas, T. Retson.
Title of the Original Case: Cerebral Arteriovenous Malformation.
Publication Date of the Original Case: 5/27/2021.
Supspecialties: Neuroradiology, Vascular Imaging, Radiation Oncology, Magnetic Resonance Imaging.
Copyright © Radiological Society of North America, Inc. (RSNA), All Rights Reserved

Question Identifier: RSNA-RadioQA-Q65

DOI of the Original Case: 10.1148/cases.20224616.
Authors of the Original Case: D. Albenda, M. Queiroz.
Title of the Original Case: Encapsulated fat necrosis.
Publication Date of the Original Case: 6/15/2021.
Supspecialties: Molecular Imaging, Radiation Oncology, Gastrointestinal, Oncologic Imaging, Nuclear Medicine.
Copyright © Radiological Society of North America, Inc. (RSNA), All Rights Reserved

Question Identifier: RSNA-RadioQA-Q66

DOI of the Original Case: 10.1148/cases.20221463.
Authors of the Original Case: R. Zeitoun, R. Merard, U. Kularatne.
Title of the Original Case: Dermatofibrosarcoma Protuberans.
Publication Date of the Original Case: 1/15/2021.
Supspecialties: Chest, Radiation Oncology, Computed Tomography, Magnetic Resonance Imaging, Oncologic Imaging, Musculoskeletal.
Copyright © Radiological Society of North America, Inc. (RSNA), All Rights Reserved

Question Identifier: RSNA-RadioQA-Q67

DOI of the Original Case: 10.1148/cases.20238226.
Authors of the Original Case: Z. LeBaron, J. Rabang, D. Gridley, A. Roh.
Title of the Original Case: Gallbladder Carcinoma.
Publication Date of the Original Case: 1/4/2023.
Supspecialties: Radiation Oncology, Magnetic Resonance Imaging, Emergency Radiology, Gastrointestinal, Ultrasound, Computed Tomography, Oncologic Imaging.
Copyright © Radiological Society of North America, Inc. (RSNA), All Rights Reserved

Question Identifier: RSNA-RadioQA-Q68

DOI of the Original Case: 10.1148/cases.20224397.
Authors of the Original Case: R. Vyas, R. Vyas, A. Singh.
Title of the Original Case: Central Nervous System Tuberculosis.
Publication Date of the Original Case: 6/7/2021.
Supspecialties: Neuroradiology.
Copyright © Radiological Society of North America, Inc. (RSNA), All Rights Reserved

Question Identifier: RSNA-RadioQA-Q69

DOI of the Original Case: 10.1148/cases.20223494.
Authors of the Original Case: H. Diep, D. Poletto.
Title of the Original Case: Osmotic demyelination syndrome.
Publication Date of the Original Case: 11/27/2020.
Supspecialties: Neuroradiology.

Question Identifier: RSNA-RadioQA-Q70

DOI of the Original Case: 10.1148/cases.20224037.

Authors of the Original Case: M. Boukoucha, R. Khelifa, A. Daghfous.

Title of the Original Case: Leptomeningeal siderosis.

Publication Date of the Original Case: 7/7/2021.

Supspecialties: Neuroradiology.

Copyright © Radiological Society of North America, Inc. (RSNA), All Rights Reserved

Question Identifier: RSNA-RadioQA-Q71

DOI of the Original Case: 10.1148/cases.20224460.

Authors of the Original Case: G. Rauch.

Title of the Original Case: BI-RADS 2 - Large rod-like calcifications.

Publication Date of the Original Case: 7/27/2021.

Supspecialties: Breast Imaging.

Copyright © Radiological Society of North America, Inc. (RSNA), All Rights Reserved

Question Identifier: RSNA-RadioQA-Q72

DOI of the Original Case: 10.1148/cases.20225300.

Authors of the Original Case: A. Griffith, R. Woods.

Title of the Original Case: Benign Breast Lipoma.

Publication Date of the Original Case: 7/27/2021.

Supspecialties: Breast Imaging.

Copyright © Radiological Society of North America, Inc. (RSNA), All Rights Reserved

Question Identifier: RSNA-RadioQA-Q73

DOI of the Original Case: 10.1148/cases.20225240.

Authors of the Original Case: A. Griffith, R. Woods.

Title of the Original Case: Axillary Adenopathy Secondary to HIV.

Publication Date of the Original Case: 11/1/2021.

Supspecialties: Breast Imaging.

Copyright © Radiological Society of North America, Inc. (RSNA), All Rights Reserved

Question Identifier: RSNA-RadioQA-Q74

DOI of the Original Case: 10.1148/cases.20223554.

Authors of the Original Case: P. Garg, A. Thakral, R. Malhotra, P. SARGAR.

Title of the Original Case: Mineralising vasculopathy with infarct.

Publication Date of the Original Case: 1/29/2021.

Supspecialties: Head and Neck.

Copyright © Radiological Society of North America, Inc. (RSNA), All Rights Reserved

Question Identifier: RSNA-RadioQA-Q75

DOI of the Original Case: 10.1148/cases.20225940.

Authors of the Original Case: A. Velasco, C. Manjarrez, M. Matos.

Title of the Original Case: TI-RADS 5.

Publication Date of the Original Case: 10/13/2021.

Supspecialties: Ultrasound, Head and Neck.

Copyright © Radiological Society of North America, Inc. (RSNA), All Rights Reserved

Question Identifier: RSNA-RadioQA-Q76

DOI of the Original Case: 10.1148/cases.20224673.

Authors of the Original Case: T. Albataineh, T. Rizvi.

Title of the Original Case: TIPIIC syndrome.

Publication Date of the Original Case: 6/28/2021.

Supspecialties: Head and Neck, Neuroradiology.

Copyright © Radiological Society of North America, Inc. (RSNA), All Rights Reserved

Question Identifier: RSNA-RadioQA-Q77

DOI of the Original Case: 10.1148/cases.20224400.

Authors of the Original Case: R. Vyas, A. Vyas, R. Vyas, A. Singh.

Title of the Original Case: Right vocal cord palsy.
Publication Date of the Original Case: 6/15/2021.
Supspecialties: Neuroradiology, Head and Neck.
Copyright © Radiological Society of North America, Inc. (RSNA), All Rights Reserved

Question Identifier: RSNA-RadioQA-Q78

DOI of the Original Case: 10.1148/cases.20225342.
Authors of the Original Case: O. Schoeck, M. Horrow, J. Ganeles, J. Gubernick.
Title of the Original Case: Putty Kidney.
Publication Date of the Original Case: 9/29/2021.
Supspecialties: Genitourinary.
Copyright © Radiological Society of North America, Inc. (RSNA), All Rights Reserved

Question Identifier: RSNA-RadioQA-Q79

DOI of the Original Case: 10.1148/cases.20221886.
Authors of the Original Case: P. Cormier, K. Ledbetter, J. Leschied, G. Sabharwal.
Title of the Original Case: Duplicated Collecting System with Vesicoureteral Reflux in the Lower Pole Moiety.
Publication Date of the Original Case: 8/12/2020.
Supspecialties: Genitourinary, Pediatric.
Copyright © Radiological Society of North America, Inc. (RSNA), All Rights Reserved

Question Identifier: RSNA-RadioQA-Q80

DOI of the Original Case: 10.1148/cases.20222850.
Authors of the Original Case: A. Rand, D. Akselrod, J. Tam.
Title of the Original Case: Schistosomiasis Bladder Wall Calcification.
Publication Date of the Original Case: 11/2/2020.
Supspecialties: Computed Tomography, Genitourinary.
Copyright © Radiological Society of North America, Inc. (RSNA), All Rights Reserved

Appendix S2

The complete ExtendedQA dataset, consisting of 24 expert-curated questions, with all the questions and their corresponding answers is as follows:

<p>Question Identifier: ExtendedQA-Q1</p> <p>Question: A 74 year-old patient presents with progressive shortness of breath over the last years. He is a former mining worker. CT shows calcified pleural plaques. What is the most likely diagnosis?</p> <p>Reference Standard Answer: Asbestosis.</p> <p>Supspecialties: Chest, Computed Tomography.</p>
<p>Question Identifier: ExtendedQA-Q2</p> <p>Question: What is considered a malignant course of the coronary arteries?</p> <p>Reference Standard Answer: Interarterial course.</p> <p>Supspecialties: Cardiac.</p>
<p>Question Identifier: ExtendedQA-Q3</p> <p>Question: What are the differential diagnoses of a solid mass in the anterosuperior mediastinum?</p> <p>Reference Standard Answer: Thymoma, thyroid (mass), lymphoma, teratoma (and germ cell tumors), thoracic aorta (e.g., aneurysm).</p> <p>Supspecialties: Chest.</p>
<p>Question Identifier: ExtendedQA-Q4</p> <p>Question: What are differential diagnoses of pulmonary cavities?</p> <p>Reference Standard Answer: Cancer, autoimmune diseases (granulomatosis with polyangiitis, rheumatoid arthritis), vascular (bland/septic emboli), infection (e.g., tuberculosis), trauma (pneumatocoles), youth (CPAM, sequestration, bronchogenic cyst); Cavity mnemonic.</p> <p>Supspecialties: Chest.</p>
<p>Question Identifier: ExtendedQA-Q5</p> <p>Question: Which MRI contrast agent can be used to detect an insufficiency of a biliary anastomosis?</p> <p>Reference Standard Answer: Eovist / Gadoteric acid or disodium.</p> <p>Supspecialties: Gastrointestinal, Magnetic Resonance Imaging.</p>
<p>Question Identifier: ExtendedQA-Q6</p> <p>Question: What are possible distributions of pulmonary nodules? Name one differential diagnosis for each distribution.</p> <p>Reference Standard Answer: Perilymphatic (e.g., sarcoidosis), centrilobular (special form: tree-in-bud; e.g., tuberculosis), diffuse (e.g., disseminated pulmonary metastasis).</p> <p>Supspecialties: Chest.</p>
<p>Question Identifier: ExtendedQA-Q7</p> <p>Question: I am looking at a prostate MRI and see a lesion in the right posterolateral peripheral zone. The lesion is hypointense in T2, hyperintense in DWI, hypointense in ADC and has a strong and early signal enhancement after contrast administration. What kind of lesion could this be?</p> <p>Reference Standard Answer: Prostate cancer.</p> <p>Supspecialties: Genitourinary, Magnetic Resonance Imaging.</p>
<p>Question Identifier: ExtendedQA-Q8</p> <p>Question: I am looking at an X-ray of the lumbar spine on a sagittal view. There are prominent endplate densities at multiple contiguous vertebral levels, leading to a sclerotic-lucent-sclerotic appearance. The Patient has a history of renal insufficiency. What is this appearance of the spine called and what is the most likely diagnosis?</p> <p>Reference Standard Answer: Rugger jersey spine; secondary hyperparathyroidism.</p> <p>Supspecialties: Musculoskeletal.</p>
<p>Question Identifier: ExtendedQA-Q9</p> <p>Question: I see a prominent pulmonary embolus in the right pulmonary artery on a CT pulmonary angiography. What are signs of right ventricular dysfunction?</p> <p>Reference Standard Answer: Abnormal position of the interventricular septum, contrast reflux into inferior vena cava/liver veins, increased diameter of the right ventricle.</p> <p>Supspecialties: Cardiac, Chest, Computed Tomography, Emergency Radiology.</p>
<p>Question Identifier: ExtendedQA-Q10</p> <p>Question: A 24 year-old patient presents with right upper quadrant pain, fever and jaundice. MRI of the liver shows T1-hypointense, T2-hyperintense, segmental dilatation of the intrahepatic bile ducts, leading to a multicystic appearance. There are multiple concrements in the intrahepatic bile ducts. The patient has no history of bowel disease. What is the most likely diagnosis?</p>

Reference Standard Answer: Caroli-disease.

Supspecialties: Emergency Radiology, Musculoskeletal.

Question Identifier: ExtendedQA-Q11

Question: I am looking at an X-ray of the knee on an anteroposterior view of a patient after trauma. I see an elliptic bone fragment projected parallel to the lateral aspect of the tibial plateau. What is the most likely diagnosis?

Reference Standard Answer: Segond fracture, indicative of a rupture of the anterior cruciate ligament.

Supspecialties: Gastrointestinal, Magnetic Resonance Imaging.

Question Identifier: ExtendedQA-Q12

Question: I see a right-sided enlarged lymph node posterolateral to the anterior belly of the digastric muscles on a CT of the neck. What is the corresponding neck lymph node level?

Reference Standard Answer: Level Ib.

Supspecialties: Computed Tomography, Head and Neck.

Question Identifier: ExtendedQA-Q13

Question: I am looking at a CT angiography of the abdomen at the arterial phase. I see a complete defect of contrast in the infrarenal aorta extending into both common iliac arteries. What is this condition called?

Reference Standard Answer: Leriche syndrome.

Supspecialties: Computed Tomography, Emergency Radiology, Vascular Imaging.

Question Identifier: ExtendedQA-Q14

Question: I see a lesion in an MRI of the liver that is hyperintense on T2 relative to the surrounding liver parenchyma, but less than the intensity of water. Upon contrast administration, the lesion shows early peripheral nodular enhancement that is shifting centripetally on delayed images. What is the most likely diagnosis?

Reference Standard Answer: Hepatic hemangioma.

Supspecialties: Gastrointestinal, Magnetic Resonance Imaging.

Question Identifier: ExtendedQA-Q15

Question: What is the most commonly used chemotherapy agent in transcatheter arterial chemoembolisation of hepatocellular carcinomas?

Reference Standard Answer: Doxorubicin.

Supspecialties: Interventional Radiology.

Question Identifier: ExtendedQA-Q16

Question: I see an adrenal lesion in an MRI of the epigastric region. The lesion demonstrates a strong signal dropout on opposed-phase images. What is the most likely diagnosis?

Reference Standard Answer: Adrenal adenoma.

Supspecialties: Gastrointestinal, Magnetic Resonance Imaging.

Question Identifier: ExtendedQA-Q17

Question: I am looking at a contrast-enhanced CT of the abdomen on the arterial phase in a patient with an infrarenal abdominal aortic aneurysm that has been treated by EVAR. I see contrast agent in the aneurysmal sac, originating from a left-sided lumbar artery. What is the most likely diagnosis?

Reference Standard Answer: Endoleak type IIa.

Supspecialties: Computed Tomography, Vascular Imaging.

Question Identifier: ExtendedQA-Q18

Question: Strongly hyperdense lesions are noted in the segmental pulmonary arteries of the right lower lobe on a non-contrast CT of the thorax. The patient has a history of vertebroplasty. What kind of lesions could that be?

Reference Standard Answer: Pulmonary cement embolism.

Supspecialties: Chest, Computed Tomography, Musculoskeletal.

Question Identifier: ExtendedQA-Q19

Question: I see a lesion in an MRI of the liver that is slightly hyperintense on T2 and hypointense on T1 relative to the surrounding liver parenchyma. The lesion shows heterogenous arterial enhancement and a washout in the venous phase. The lesion shows a central scar on T2w imaging. What is the most likely diagnosis?

Reference Standard Answer: Fibrolamellar hepatocellular carcinoma.

Supspecialties: Gastrointestinal, Magnetic Resonance Imaging.

Question Identifier: ExtendedQA-Q20

Question: I see prominent endplate densities at multiple contiguous vertebral levels on a sagittal X-ray of the spine and a well-defined lesion of the sixth rib on a chest X-ray. What is the most likely underlying condition?

Reference Standard Answer: Hyperparathyroidism (Rugger-Jersey-Spine and 'brown tumor').

Supspecialties: Chest, Musculoskeletal.

Question Identifier: ExtendedQA-Q21

Question: After application of contrast agent into a percutaneous transhepatic biliary drainage, portal vein branches distal to the biliary entry of the drainage show contrast enhancement. What is the most likely diagnosis?

Reference Standard Answer: Portobiliary fistula.

Supspecialties: Gastrointestinal, Magnetic Resonance Imaging.

Question Identifier: ExtendedQA-Q22

Question: I see densely sclerotic endplates in a sagittal X-ray of the spine of a 14 year old patient. What is the most likely diagnosis?

Reference Standard Answer: Osteopetrosis.

Supspecialties: Musculoskeletal, Pediatric.

Question Identifier: ExtendedQA-Q23

Question: I see mixed opacified and unopacified blood in the IVC at and cranial of the renal veins after on a abdominal CT scan at an early contrast phase after i.v. contrast application. The infrarenal vena cava appears mostly unopacified. What is the most likely diagnosis?

Reference Standard Answer: Contrast flow phenomenon in inferior vena cava (artifact).

Supspecialties: Computed Tomography, Vascular Imaging.

Question Identifier: ExtendedQA-Q24

Question: I see a synovial mass on a knee MRI. The mass is T1 and T2 hyperintense. There is a concomitant joint effusion. What is the most likely diagnosis?

Reference Standard Answer: Lipoma arborescens.

Supspecialties: Magnetic Resonance Imaging, Musculoskeletal.

Appendix S3

Glossary of Technical Terms

Tokens:

In language models, *tokens* are small units of text (often words or subwords) used by the model to process, represent, or generate text. For example, the sentence “MRI is a diagnostic tool” might be split into tokens like [“MRI”, “is”, “a”, “diagnostic”, “tool”].

Vector Representations:

A *vector representation* (sometimes called an “embedding”) is a way to translate text, images, or other data into a series of numerical values—often stored as a list or “vector”—such that similar content has similar numerical patterns. This allows algorithms to mathematically compare the semantic meaning of different inputs.

Text Embedding:

A *text embedding* is a type of vector representation specifically designed for linguistic content. It encodes each text chunk into a fixed-dimensional vector space such that texts with related meanings end up closer together in that space

Vector Database:

A *vector database* is a specialized data management system optimized for storing and retrieving vector representations. Traditional databases store and index discrete data types (like numbers or strings), whereas a vector database is designed to handle operations like *similarity search* (for instance, retrieving the closest vectors to a particular query vector).

Appendix S4

Time Comparison Between Conventional QA and RadioRAG-powered QA

The time required for question answering (QA) varies depending on the model used and the retrieval approach. Below, we provide an estimate of the time differences between conventional QA and RadioRAG-powered QA, as observed in our experiments using the RSNA-RadioQA dataset.

Conventional QA:

For conventional QA, the time required is primarily dependent on the LLM's response time. For instance, when using GPT-4 through the OpenAI API, it took approximately 30 seconds per question to generate a response.

RadioRAG-powered QA:

RadioRAG introduces additional steps for retrieving and processing relevant context before querying the LLM, which increases the total time. This process consists of the following steps:

- **Key-phrase extraction:** Approximately 10 seconds, dependent on internet speed.
- **Searching Radiopaedia using key-phrases:** Approximately 30 seconds, dependent on both internet speed and the response time of the Radiopaedia website.
- **Database creation and embedding:** With the collection of around 25 articles, this step took approximately 40 seconds, influenced by the hardware resources available.
- **LLM response generation:** This step took approximately 35 seconds, similar to conventional QA.

In total, RadioRAG-powered QA took approximately 115 seconds per question using GPT-4, about four times longer than conventional QA (30 seconds).